Project 2534 | July 2026

SJSU SAN JOSÉ STATE UNIVERSITY

MTI MINETA TRANSPORTATION INSTITUTE

Automated Battery Management Systems for Electric Vehicles

Woonki Na, PhD
Yuanyuan Xie, PhD

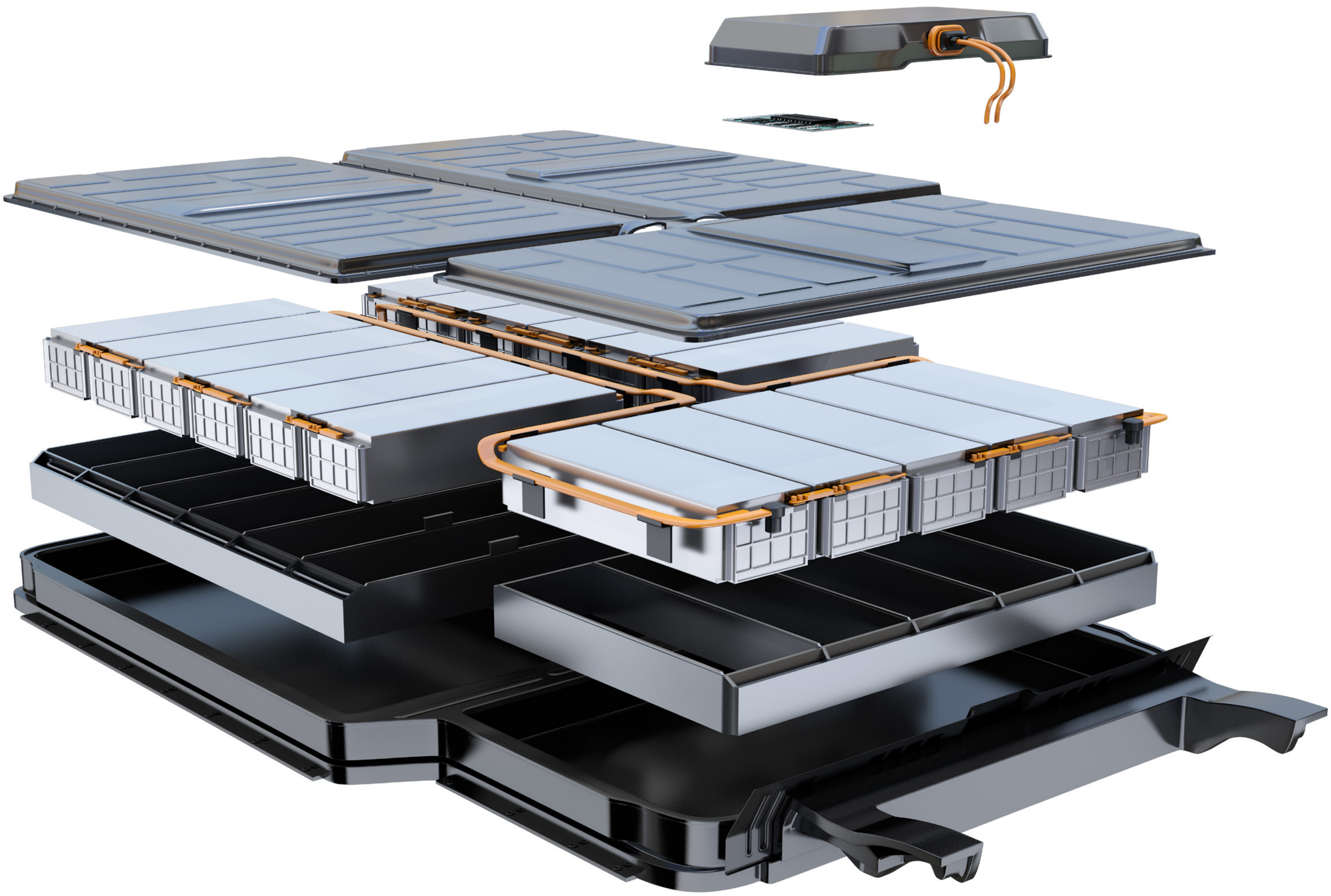

CSUTC California State University Transportation Consortium

FRESNO STATE

MINETA TRANSPORTATION INSTITUTE

Founded in 1991, the Mineta Transportation Institute (MTI), an organized research and training unit in partnership with the Lucas College and Graduate School of Business at San José State University (SJSU), increases mobility for all by improving the safety, efficiency, accessibility, and convenience of our nation's transportation system. Through research, education, workforce development, and technology transfer, we help create a connected world. MTI leads the California State University Transportation Consortium (CSUTC) funded by the State of California through Senate Bill 1 and the Climate Change and Extreme Events Training and Research (CCEETR) Program funded by the Federal Railroad Administration. MTI focuses on three primary responsibilities:

Research

MTI conducts multi-disciplinary research focused on surface transportation that contributes to effective decision making. Research areas include: active transportation; planning and policy; security and counterterrorism; sustainable transportation and land use; transit and passenger rail; transportation engineering; transportation finance; transportation technology; and workforce and labor. MTI research publications undergo expert peer review to ensure the quality of the research.

Education and Workforce Development

To ensure the efficient movement of people and goods, we must prepare the next generation of skilled transportation professionals who can lead a thriving, forward-thinking transportation industry for a more connected world. To help achieve this, MTI sponsors a suite of workforce development and education opportunities. The Institute supports educational programs offered by the Lucas Graduate School of Business: a Master of Science in Transportation Management, plus graduate certificates that include High-Speed and Intercity Rail Management and Transportation Security Management. These flexible programs offer live online classes so that working transportation professionals can pursue an advanced degree regardless of their location.

Information and Technology Transfer

MTI utilizes a diverse array of dissemination methods and media to ensure research results reach those responsible for managing change. These methods include publication, seminars, workshops, websites, social media, webinars, and other technology transfer mechanisms. Additionally, MTI promotes the availability of completed research to professional organizations and works to integrate the research findings into the graduate education program. MTI's extensive collection of transportation-related publications is integrated into San José State University's world-class Martin Luther King, Jr. Library.

Report 26-20

Automated Battery Management Systems for Electric Vehicles

Woonki Na, PhD
Yuanyuan Xie, PhD

July 2026

A publication of the
Mineta Transportation Institute
Created by Congress in 1991

College of Business
San José State University
San José, CA 95192-0219

Technical Report Documentation Page

1. Report No.
26-20

2. Government Accession No.

3. Recipient's Catalog No.

4. Title and Subtitle
Automated Battery Management Systems for Electric Vehicles

5. Report Date
August 2026

6. Performing Organization Code

7. Authors
Woonki Na, PhD
Yuanyuan Xie, PhD

8. Performing Organization Report
CA-MTI-2534

9. Performing Organization Name and Address
Mineta Transportation Institute
College of Business
San José State University
San José, CA 95192-0219

10. Work Unit No.

11. Contract or Grant No.
SB1-SJAUX_2023-26

12. Sponsoring Agency Name and Address
State of California SB1 2017/2018
Trustees of the California State University
Sponsored Programs Administration
401 Golden Shore, 5th Floor
Long Beach, CA 90802

13. Type of Report and Period Covered

14. Sponsoring Agency Code

15. Supplemental Notes
10.31979/mti.2026.2534

16. Abstract
Electric vehicle (EV) safety, efficiency, and lifetime are strongly influenced by how well battery cells are managed, and as EV adoption accelerates, improving battery performance has become critical to vehicle reliability, cost, and public trust. This report conducts a field study on the core technologies and challenges in Battery Management Systems (BMS), focusing on the classification of BMS circuit topologies (design/structures) and systematically reviewing different topologies of active cell balancing circuits (systems that move energy from stronger battery cells to weaker ones). The study provides a detailed analysis of the working principles, advantages, and disadvantages of various active balancing circuit topologies. Additionally, it elaborates on the key algorithms underpinning battery balancing. The report also examines the main challenges in designing these systems, including balancing efficiency, cost, reliability, and the ability to scale. It also highlights the difficulty of accurately understanding battery conditions and making real-time decisions as operating conditions change. The study also summarizes and reviews major breakthroughs in balancing algorithms within the field. By conducting comprehensive research on circuit topologies and core algorithms, this report informs the design and performance optimization of BMS, particularly active balancing systems. Addressing these challenges is essential to improving EV safety, reducing costs, and supporting the broader adoption of electric vehicles.

17. Key Words
Battery management system, active cell balancing

18. Distribution Statement
No restrictions. This document is available to the public through The National Technical Information Service, Springfield, VA 22161.

19. Security Classif. (of this report)
Unclassified

20. Security Classif. (of this page)
Unclassified

21. No. of Pages
56

22. Price

Form DOT F 1700.7 (8-72)

DOI: 10.31979/mti.2026.2534

Mineta Transportation Institute
College of Business
San José State University
San José, CA 95192-0219

Email: mineta-institute@sjsu.edu

transweb.sjsu.edu/research/2534

Acknowledgments

This work was supported by the Fresno State Transportation Institute (FSTI). The authors would like to thank FSTI and the Fresno County Transportation Authority for their financial support through the Measure C New Technology Reserve Program.

Contents

List of Figures

List of Tables

Executive Summary

Modern electric vehicles depend on battery packs containing hundreds of lithium-ion cells that must work in precise coordination. When individual cells charge and discharge at different rates—a condition called cell imbalance—the pack loses usable energy, degrades faster, and risks dangerous overheating. To address this, the research team investigated Battery Management Systems (BMS) that utilize "active cell balancing," a process that physically redistributes energy between cells rather than wasting excess charge as heat. This study aims to provide automotive engineers and EV manufacturers with a technical framework for selecting balancing systems that maximize battery life and safety. As California accelerates toward its zero-emission vehicle mandates and federal investment in EV infrastructure expands across the United States, optimizing battery management systems has become a critical engineering and transportation policy priority with direct implications for grid resilience, vehicle reliability, and public confidence in electrified transportation.

The research team systematically analyzed the core engineering challenges of BMS design, specifically the trade-offs between circuit complexity, performance, and cost. Using detailed simulations, the team compared three primary topologies in terms of the electrical system layout of the electronic components. These included switched-capacitor designs, inductor-based systems, and Dual Active Bridge (DAB) converter architectures.

The findings reveal that while switched-capacitor designs are cost-effective, they transfer energy too slowly for high-performance packs. In contrast, the research team identified the DAB converter as the superior solution for demanding applications; it enables bidirectional energy flow and galvanic isolation which is a critical safety barrier while achieving energy transfer efficiencies exceeding 90%.

The study concludes that because no single topology is universally optimal, engineers must weigh specific performance targets against system complexity. These results offer practical selection guidance for the next generation of electric vehicle development, emphasizing that successful BMS implementation requires integrated innovation at both circuit and control algorithm levels. In parallel with the simulation work, the research team has initiated an empirical battery testing program. Cell preconditioning and baseline characterization are complete, and self-discharge screening of NiMH cells has successfully identified degraded cells for constructing intentionally imbalanced modules. Self-discharge and impedance testing of Li-ion cells is currently ongoing. Active balancing trials comparing all three topologies under hardware conditions are the immediate next step; full results will be reported in future work. These hardware findings will provide empirical validation of the simulation results summarized above.

1. Introduction

The global transition toward sustainable energy has positioned lithium-ion (Li-ion) batteries as the cornerstone of modern electrification. From the high-torque requirements of electric vehicles (EVs) to the massive scale of battery energy storage systems (BESS), the demand for high-density energy storage is unprecedented (IEA 2024). However, as battery packs grow in size and complexity, often comprising hundreds or thousands of individual cells, maintaining pack health and operational safety becomes a significant engineering challenge (Attia et al. 2025). In a series-connected battery string, the total performance is strictly limited by the "weakest" cell. According to Hein et al. (2023), factors such as manufacturing tolerances, uneven thermal distribution, and chemical aging lead to inherent variations in cell capacity and internal resistance. Without intervention, these discrepancies result in "cell unbalance," where individual cells reach their voltage limits prematurely, leaving the rest of the pack underutilized and potentially leading to hazardous conditions such as thermal runaway (Feng et al. 2020).

These challenges are acutely relevant to California and the United States as whole, where electrification targets and the scale of EV deployment make battery management system performance a transportation policy priority, not merely an engineering concern. California's Advanced Clean Cars II regulation mandates that all new passenger vehicles sold in the state be zero-emission by 2035 (Pickett 2024), and federal investment through the Bipartisan Infrastructure Law has committed over $7.5 billion to nationwide EV charging infrastructure, requiring comprehensive grid deployment planning (Bennett 2024; Wood et al. 2023). At the same time, the California Energy Commission and the California Air Resources Board have identified battery degradation and range anxiety as primary barriers to consumer adoption of EVs among lower-income and rural populations—communities that are disproportionately represented in the Central Valley regions served by the Fresno State Transportation Institute, which sponsors this research.

As EV penetration increases across California's diverse driving environments—from the high-temperature conditions of the San Joaquin Valley to the high-altitude cold of the Sierra Nevada—the cell imbalance mechanisms described above are intensified: thermal extremes accelerate differential aging, widen cell-to-cell resistance gradients, and increase the frequency and severity of balancing demands. Advancing BMS active balancing technology is therefore directly relevant to California's transportation electrification goals, to the reliability of the state's growing EV fleet, and to the federal objective of building a resilient, domestically managed electric vehicle supply chain. This report's findings on topology selection and control algorithm design are intended to provide actionable technical guidance for engineers, procurement agencies, and policymakers operating within this California and U.S. context.

To mitigate these issues, the battery management system (BMS) must employ equalization strategies. While traditional passive balancing methods are prevalent due to their low cost, they dissipate excess energy as heat through shunt resistors. This increases thermal management requirements and reduces overall system efficiency (Ashraf, Ali, and Sunjury 2025). Consequently, there has been a paradigm shift toward active cell balancing, which utilizes energy-shunting mechanisms to redistribute charge between cells rather than wasting it (Safari et al. 2025).

Active balancing is primarily achieved through sophisticated power electronics topologies, including inductive, capacitive, and power converter-based architectures. As detailed in the latest comprehensive review by Ashraf, Ali, and Sunjury (2025), the selection of an equalization circuit is now a multi-objective optimization problem that must balance hardware complexity, weight, and energy recovery efficiency. Furthermore, modern trends are moving beyond static circuit design toward "intelligent" balancing, where machine learning and Digital Twin technologies are used to manage the non-linear switching stresses of these power electronics systems (Njoku et al. 2025; Bai et al. 2024). The evolution of cell balancing has progressed from simple resistive dissipation to complex high frequency switching converters.

This section reviews the literature regarding the three primary power electronics categories used in active balancing: Capacitor-Based Topologies, Inductor-Based Topologies, and DC-to-DC Converter Topologies (Li et al. 2025; Zhao et al. 2023).

The remainder of this report is structured as follows. Section 1 (this section) surveys the three principal power electronics topologies employed in active cell balancing—capacitor-based, inductor-based, and DC-to-DC converter-based—with the goal of identifying the engineering trade-offs that motivate the selection criteria examined later in the report. This critical survey of the literature directly motivates Section 2, which moves from taxonomy to performance analysis: building on the trade-offs identified in the review, Section 2 quantifies balancing speed, energy efficiency, and control complexity for each topology under dynamic conditions representative of real-world EV drive cycles using high-fidelity MATLAB/Simulink simulations. The simulation findings, in turn, establish specific performance hypotheses—for instance, that DAB converter-based balancing achieves superior state-of-charge convergence rates and efficiency at the cost of greater control complexity—that are then subjected to empirical validation in Section 3. Section 3 describes the authors' ongoing hardware testing program, including cell preconditioning, self-discharge screening, impedance characterization, and module-level cycling trials. Although the full empirical dataset is still being collected, the preliminary results presented confirm cell-to-cell consistency in the preconditioned population and establish the experimental baseline against which the topology-by-topology comparisons from Section 2 will be validated. Section 4 summarizes the findings across all three stages and provides practical selection guidance for automotive engineers and EV system designers, with particular attention to California and U.S. deployment contexts.

1.1 Capacitor-Based Topologies

Ye and Cheng (2016) focused on Switched-Capacitor (SC) circuits, which act as a bridge to move electricity between cells. In this design, a capacitor is used to move small amounts of charge by flipping back and forth between a cell with a higher voltage and one with a lower voltage using electronic switches. The challenge of maintaining a healthy battery pack begins with the reality that no two cells are perfectly identical. Minor variations in internal resistance and aging cause some cells to charge or discharge faster than their neighbors, which is critical because a series-connected pack is only as strong as its weakest cell. To solve this, researchers use active balancing circuits to physically relocate energy from the strongest cells to the weakest ones, ensuring the entire system reaches its full potential (Li et al. 2025; Zhao et al. 2023).

One common method for this transfer is the switched capacitor approach, which functions like an automated "bucket brigade." A capacitor acts as an intermediate medium that picks up charge from a high-voltage cell and drops it off at a lower-voltage cell. This technique is highly valued in industry because it is relatively inexpensive and avoids the complex sensors or heavy magnetic components required by other balancing systems (Li et al. 2025; Zhao et al. 2023).

The most fundamental version of this technology is the Fixed Switched Capacitor (FSC) (Ye and Cheng 2016). This system relies on a basic "on–off" timing signal to flip switches at a constant rate. While simple to implement, it faces a physical limitation: as cells reach a balanced state, the voltage difference—and thus the electrical "pressure"—disappears. This causes the flow of electricity to drop off sharply, making the FSC method increasingly slow and inefficient for the large battery systems used in modern electric vehicles (Li et al. 2025; Zhao et al. 2023).

To overcome these hurdles, researchers developed the Resonant Switched Capacitor (RSC) topology (Li et al. 2025; Zhao et al. 2023). By adding a small inductor to the circuit, they create a resonant tank that allows for a technique called Zero-Current Switching (ZCS) (Erickson & Maksimovic 2001). This allows the transistors to turn on and off exactly when the current hits zero. By switching at these precise moments, the RSC model minimizes energy loss, generates significantly less heat, and reduces the electrical noise that can disrupt sensitive electronics during the balancing process (Li et al. 2025; Zhao et al. 2023).

1.2 Inductor-Based Topologies

Inductor-based balancing represents a significant step forward in power electronics complexity. Unlike capacitor-based systems that rely on voltage differences to move charge, inductors use magnetic fields to "force" energy transfer. This capability allows them to "step up" or "step down" voltage, making them much more effective at moving energy across large battery strings.

Inductive balancing systems are generally categorized by the number of magnetic components used to manage energy. The simplest version is the single-inductor system, favored for its low cost and small physical footprint. In this setup, one inductor is responsible for transferring charge across the entire battery string. While this reduces hardware complexity, it is often too slow for modern electric vehicles because the inductor must handle cells sequentially, significantly extending the time needed to reach equilibrium (Li et al. 2025; Zhao et al. 2023).

To solve these speed bottlenecks, multi-inductor systems utilize several components to enable parallel balancing. This allows multiple cell pairs to exchange energy simultaneously, making the process much faster and more suitable for large-scale applications (Song, Hredzak, and Fletcher 2025). However, this performance boost requires more circuit board space and increases the overall cost of the BMS. More advanced inductive balancers use transformers instead of simple inductors. The two most common types are flyback and forward converters, which are especially important for high-voltage systems, such as the 800V architectures used in high-performance EVs (Ashraf, Ali, and Sunjury 2025; Deshmukh et al. 2024).

A key advantage of using transformers is galvanic isolation. This safety feature creates a physical and electrical barrier between the individual battery cells and the rest of the balancing system. If a fault or short circuit occurs in one cell, the isolation prevents that high voltage from spreading through the entire system and causing a catastrophic failure (Ashraf, Ali, and Sunjury 2025). However, while transformer-based designs currently deliver the fastest "cell-to-pack" balancing speeds, they are subject to clear efficiency trade-offs. As noted by Ashraf, Ali and Sunjury (2025), a portion of the transferred energy is inevitably dissipated as waste heat due to magnetic core losses. These losses occur as the magnetic field inside the transformer core continuously alternates during high-frequency operation, introducing an upper limit to the system's net efficiency.

1.3 DC-to-DC Converter-Based Topologies

The most versatile category of active balancing involves specialized DC-to-DC converter architectures, such as buck-boost, cuk, and septic converters, which function as intelligent power adjusters to precisely regulate electricity flow between different sections of a battery system. Unlike simpler balancing circuits, these topologies, specifically bi-directional buck-boost converters and modular multi-level converters (MMCs), provide granular control over voltage and current, resulting in high operational efficiency (Li et al. 2025; Zhao et al. 2023). Among these, the bi-directional buck-boost converter is currently the most widely cited and utilized topology in active balancing research due to its versatile dual-path energy transfer capability. This bi-directional functionality enables "cell-to-pack" (C2P) balancing, where excess energy is taken from a high-voltage cell and redistributed to the rest of the string, as well as "pack-to-cell" (P2C) balancing, which draws energy from the entire pack to "top up" a lagging cell. By strategically moving energy exactly where it is required, these converters prevent individual cells from being overstressed, which significantly extends the overall lifespan of the battery pack (Li et al. 2025).

Beyond individual cell management, recent literature suggests that modular multi-level converters (MMCs) represent the future of grid-scale storage systems. These advanced architectures integrate the balancing function directly into the power conversion stage of the inverter, effectively merging the battery management and power delivery processes. By doing so, MMCs can eliminate the need for separate, dedicated balancing hardware, thereby reducing the overall footprint and complexity of large-scale energy storage installations. This integration of balancing and conversion stages is increasingly viewed as a critical step toward more efficient and reliable high-voltage battery management in industrial plants and electric utility infrastructure (Ashraf, Ali, and Sunjury 2025).

1.4 The Present Study

In this study, a comprehensive performance analysis of active cell balancing architectures was conducted to evaluate the operational efficacy of various automated topologies. While extant literature frequently characterizes balancing performance under steady-state or equilibrium conditions, this analysis subjects capacitive and converter-based architectures to dynamic, high-fidelity electric vehicle (EV) drive cycles. These simulated environments replicate the non-linear current demands and rapid state-of-charge (SoC) fluctuations inherent in real-world automotive applications.

Notably, this study *focuses* specifically on the trade-offs between low-cost capacitive "shuttling" and high-performance converter-based "regulation." While capacitive balancing systems are historically significant, they are often omitted in favor of converter-based architectures in modern research due to the superior controllability and bidirectional efficiency of converters.

By quantifying the critical trade-offs between equalization latency (balancing speed), energy recovery efficiency, and computational overhead, this work establishes a rigorous performance benchmark for next-generation automated energy management systems. The findings serve to identify the optimal hardware-software configurations required to mitigate cell-to-cell variance in high-capacity lithium-ion battery packs.

2. Active Cell Balancing Methods

Active cell balancing encompasses a range of circuit-based approaches, each utilizing distinct components and mechanisms to redistribute energy across a battery pack. This chapter examines three primary topologies—capacitor-based, inductor-based, and DC-to-DC converter-based systems—analyzing their operational principles, performance strengths, and the inherent trade-offs regarding balancing speed, efficiency, and hardware complexity. Understanding these distinctions is essential for selecting the most appropriate balancing architecture for a specific application.

2.1 Capacitor-Based Cell Balancing

The fundamental structure of the ladder-based switched-capacitor balancer features series-connected battery cells (B_1 through B_4) and "flying" capacitors (C_1 through C_3) as presented in Figure 1.

Figure 1. Capacitive-Based Cell Balancing Scheme

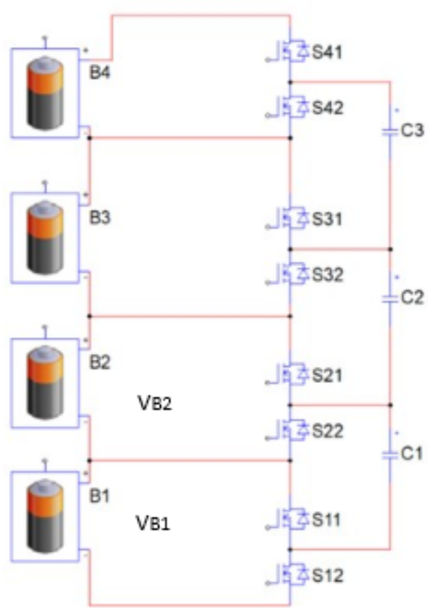

This topology is well known for its autonomous nature (Ye and Cheng 2016), as it does not inherently require a centralized processor to determine which cell requires balancing. Instead, the hardware relies on high-frequency switching to move charge from areas of high potential to areas of low potential.

The system operates via synchronized pulse width modulation (PWM) signals controlling half-bridge MOSFET (Metal–Oxide–Semiconductor Field-Effect Transistor) pairs (Erickson and Maksimovic 2001), denoted in the schematics as S_{n1} and S_{n2} (n:1~4). These switches are toggled at a fixed high frequency to alternate the connection of the flying capacitors across the battery string. The simplicity of this control logic makes it an attractive candidate for cost-sensitive applications where extreme balancing speed is not the primary requirement.

The balancing mechanism follows a specific two-phase "shuttle" logic during operation. In the first phase, known as charge acquisition, the top switches turn ON to connect the flying capacitor in parallel with a specific cell, allowing it to harvest excess charge. In the subsequent phase, the PWM signal reverses to turn ON the bottom switches, shifting the capacitor in parallel with the adjacent lower-potential cell to discharge that stored energy.

The ladder-type switched-capacitor architecture offers a distinct set of operational trade-offs that makes it suitable for specific battery management applications while limiting its effectiveness in others. One of the primary advantages of this method is its high energy efficiency compared to traditional passive balancing (Li et al. 2025; Zhao et al. 2023). Rather than dissipating excess energy as heat through resistors, the SC method redistributes charge dynamically from high-voltage cells to low-voltage cells, preserving the total energy within the pack. This process is supported by relatively simple control logic; the system utilizes fixed PWM signals for half-bridge pairs, effectively eliminating the requirement for high-resolution sensing or sophisticated micro-processing units.

Furthermore, the architecture benefits from low voltage stress on its internal components. Because capacitors and MOSFET switches are connected across adjacent cells, they only need to be rated for the voltage of a single cell plus a standard safety margin, which can simplify the bill of materials for lower-voltage strings. This leads to a largely autonomous operation, where balancing occurs naturally as long as a voltage differential exists between neighbors. This "self-regulating" behavior is governed by the circuit's inherent exponential charge transfer characteristics.

However, these benefits are countered by several significant disadvantages that impact performance in high-capacity electric vehicle (EV) packs. The most prominent issue is the slow equalization speed caused by the sequential nature of the ladder architecture (Li et al. 2025; Zhao et al. 2023). Energy must "hop" from one cell to the next in a bucket-brigade fashion; consequently, moving charge from the first cell to the last in a large-scale pack requires considerable time, which may be insufficient during rapid dynamic driving cycles.

This latency is compounded by the current reduction at equilibrium. For example, as cell voltages V_{B1} and V_{B2} for cell B1 and B2, respectively, in Figure 1 converge and the potential difference between V_{B1} and V_{B2} nears zero, the balancing current decreases exponentially, making it technically difficult to reach absolute equilibrium in a time-efficient manner. Finally, the hardware footprint is a concern for compact BMS designs. For a string of N cells, the system requires 2N switches and N - 1 capacitors, a high component count that increases both the physical volume and the overall cost of the battery management hardware (Li et al. 2025; Zhao et al. 2023).

2.2 Inductor-Based Cell Balancing

The core of this system shown in Figure 2: a single inductor L is shared between two cells (B_1 and B_2) with two MOSFET switches (S_1 and S_2).

Figure 2. Inductor-Based Cell Balancing

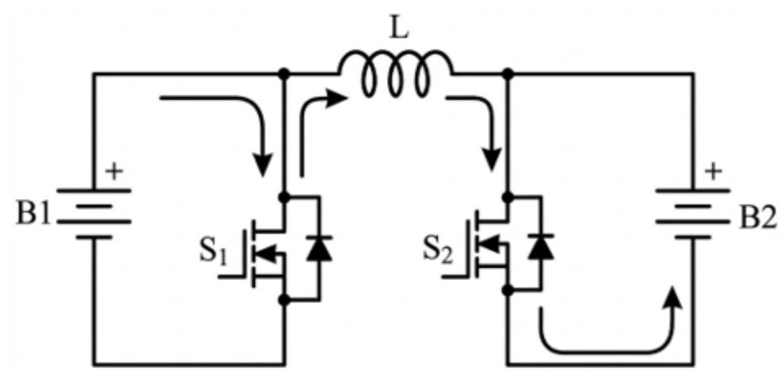

The operational cycle of an inductive balancing system begins with the charge phase, where energy is stored within the magnetic field of the component. Assuming the voltage of cell B_1 is greater than B_2, the control logic turns switch S_1 on while keeping S_2 off. During this interval, current flows directly from the higher-voltage cell B_1 through the inductor, causing the inductor current to increase linearly as it builds a magnetic charge.

Once sufficient energy is stored, the system enters the discharge phase. In this step, S_1 is turned off and S_2 is turned on, or its anti-parallel diode begins to conduct. This change in state forces the inductor to release its stored magnetic energy as current into the lower-voltage cell B_2, effectively completing the transfer of charge from the stronger cell to the weaker one. When extending this principle to a multiple-cell balancing architecture, the system utilizes a ladder inductive structure that mirrors the modular design of switched-capacitor versions as seen in Figure 3 (Ashraf, Ali, and Sunjury 2025).

Figure 3. Inductor-Based Multiple-Cell Balancing (Ashraf, Ali, and Sunjury 2025)

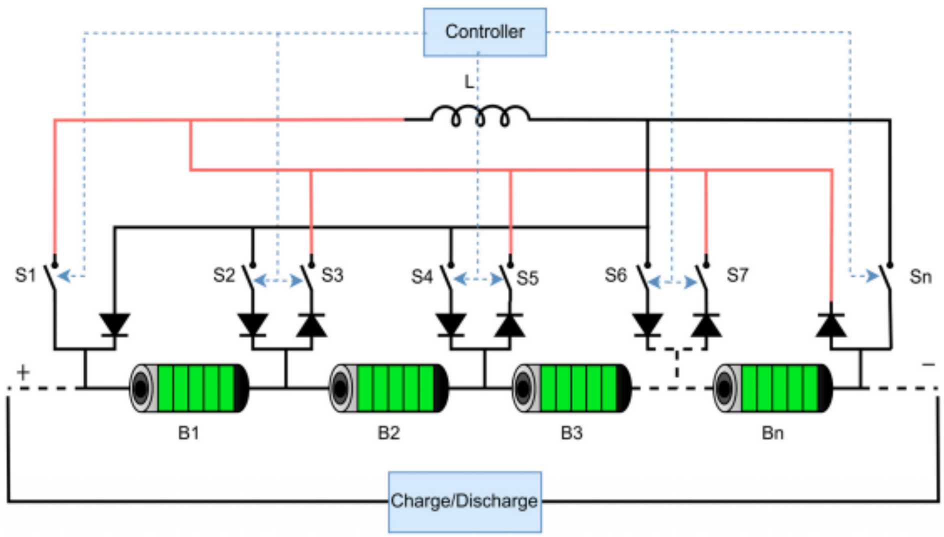

To manage multiple cells simultaneously, the architecture employs interleaved control, using synchronized pulses to move charge across multiple cell gaps at once. Unlike the exponential current curves seen in capacitive systems, the current in an inductive ladder consists of triangular ramps that rise during the charging phase and fall during discharge. The timing and logic for these synchronized pulses are critical to the system's efficiency. Specifically, the implementation of "dead time"—a brief period where both switches in a pair are turned off—is mandatory to prevent "shoot-through" conditions, where two battery cells are accidentally shorted together.

More advanced active architectures utilize transformers to achieve the galvanic isolation critical for high-voltage (800V) electric vehicle systems (Li et al. 2025; Zhao et al. 2023). This isolation establishes a vital safety barrier, preventing localized cell faults from propagating through the wider balancing system. However, these magnetic designs introduce core losses that dissipate energy as heat. Compared to capacitive methods, inductive topologies provide significantly higher equalization speeds and sustain constant balancing currents even at minimal cell-voltage differentials, though they introduce penalties in volumetric bulk and electromagnetic interference (EMI).

Managing these inductive and transformer-based networks requires complex, multi-phase switching strategies. For multi-cell architectures, synchronized pulse-width modulation (PWM) drives simultaneous charge distribution across non-adjacent cells. To mitigate the severe risk of cell short-circuits during these high-speed transitions, the control framework must implement precise dead-time allocation to prevent shoot-through currents (Ashraf, Ali, and Sunjury 2025).

2.3 DC-to-DC- Converter-Based Cell Balancing

The Dual Active Bridge (DAB) DC-to-DC converter has emerged as a premier candidate for active balancing topologies in high-capacity energy storage systems (Li et al. 2025; Zhao et al. 2023). Its prominence in recent literature is primarily attributed to its native support for bidirectional power flow, the inherent safety provided by galvanic isolation, and its capacity for high-precision controllability. Unlike capacitive "shuttle" methods that rely on natural potential gradients, the DAB system operates as an active regulator that can forcibly move energy between domains regardless of the voltage difference. This report evaluates a DAB-based balancing system designed for a series-connected four-cell lithium-ion battery pack, focusing on the architectural nuances and control logic that define its performance.

Figure 4. Dual Active Bridge (DAB) DC–to– DC converter

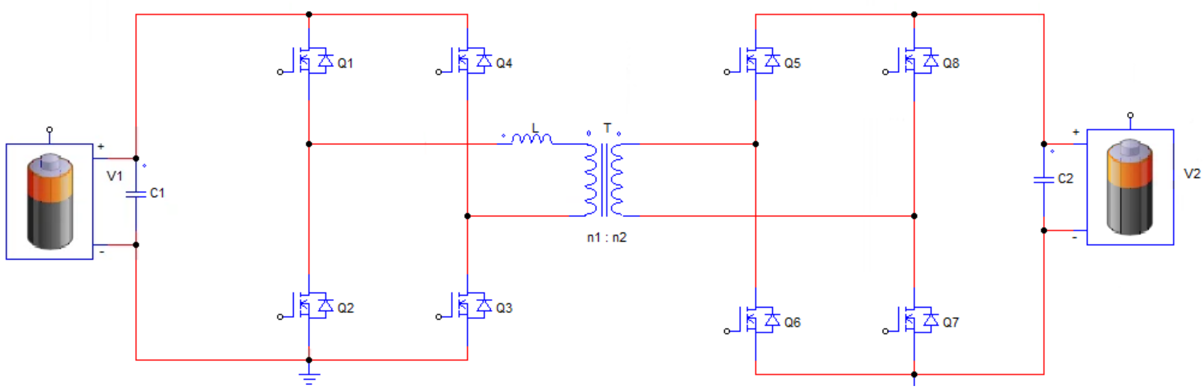

The structural foundation of the DAB converter consists of two full-bridge MOSFET networks linked by a high-frequency transformer and a series leakage inductor, as shown in Figure 4. The primary side is interfaced with the source cell or pack, while the secondary side is connected to the target load or recipient cell string. During circuit operation, the MOSFETs on each bridge are driven by square-wave signals, typically at a 50% duty cycle, to convert the DC battery voltage into a high-frequency AC signal. This AC signal is coupled through the transformer, providing an isolated path for charge redistribution. The transformer's turns ratio (n_1:n_2) allows the BMS to match differing voltage levels across the pack, which is critical when performing cell-to-pack or pack-to-cell transfers.

The operating principle relies on phase-shift modulation (Muhammetoglu and Jamil 2024) to dictate the magnitude and direction of the balancing current. By shifting the phase angle, ψ, between the primary and secondary square waves, the BMS controls the voltage drop across the series inductor, which in turn defines the current waveform. When the primary bridge leads to the secondary, energy flows toward the target; conversely, a lagging phase reverses the flow. The resulting current and voltage waveforms are characterized by trapezoidal or triangular profiles depending on the specific modulation depth. This phase control ensures that the balancing current remains constant and regulated, effectively bypassing the "current decay" issue seen in switched-capacitor systems as they approach equilibrium.

From a control standpoint, the balancing logic is managed by a centralized processor that monitors individual cell voltages and determines the optimal energy redistribution path. The control algorithm utilizes the phase shift as the primary control variable to maintain high efficiency and thermal stability. In advanced implementations, the BMS might employ Triple-Phase-Shift (TPS) control (Muhammetoglu and Jamil 2024) to optimize the internal duty cycles of the bridges, ensuring that the MOSFETs operate under zero-voltage switching (ZVS) conditions (Li et al. 2025). This sophisticated balancing logic allows the four-cell pack to reach a State of Charge (SoC) uniformity rapidly, minimizing the I^2R losses related to resistors and maximizing the lifespan of the electrochemical cells through precise, software-defined energy regulation.

Power Stage Components

The architectural core of the DAB converter is defined by two symmetrical full-bridge (H-bridge) converters, which facilitate bidirectional energy transfer through a multi-stage power conversion process. As illustrated in the system schematic of Figure 4, the primary side bridge is responsible for inverting the input DC voltage, V_1 into a high-frequency AC signal, while the secondary side bridge performs the synchronous rectification of this AC signal back into the output DC voltage, V_2. This switching action is executed by eight N-channel Metal-Oxide-Semiconductor Field-Effect Transistors (MOSFETs), denoted as Q_1 through Q_8, which are preferred over insulated-gate bipolar transistors (IGBTs) in modern battery management systems due to their superior switching speeds and significantly lower switching losses during high-frequency operation (Pascual and Krein 1997).

Central to the converter's performance and safety is the high-frequency transformer, which provides essential galvanic isolation while utilizing its turns ratio (n_1:n_2) to match voltage levels between different cells or segments of the battery pack. The actual mechanism of energy transfer is mediated by the series inductor (L), which often incorporates the transformer's inherent leakage inductance. This inductor serves as the critical energy storage element, where the magnitude of power transferred is regulated by the phase shift between the two H-bridges. To ensure the quality of the redistributed energy, an output filter capacitor (C) is integrated to smooth high-frequency ripples, thereby maintaining a stable and steady voltage across the load or the recipient battery cell.

Control Mechanism

The DAB converter achieves precise voltage regulation and efficient charge distribution through a closed-loop feedback strategy. The process begins with continuous measurement of the output voltage V_2, which is fed back to a summing point and compared against a pre-defined reference voltage, V_{ref}. This comparison generates an error signal processed by a proportional–integral (PI) controller (Muhammetoglu and Jamil 2024). The PI controller calculates the exact phase-shift angle ψ needed to eliminate the discrepancy between actual and target voltages. This value is passed to a single-phase-shift (SPS) pulse modulator, which generates high-speed gate signals for MOSFETs Q1 through Q8 as shown in Figure 4.

Replacing passive rectifiers with these controlled switches enables efficient bidirectional power transfer across the entire battery string. This symmetrical architecture provides the software-defined agility necessary to manage rapid state-of-charge fluctuations in demanding electric vehicle environments. During sudden events, such as rapid acceleration or regenerative braking, the controller modulates energy transfer at a granular level to instantly stabilize voltage sags or spikes, ensuring the pack remains balanced under extreme load and extending cell lifespan.

Figure 5. Dual Active Bridge (DAB) DC–DC Converter Operation for BMS

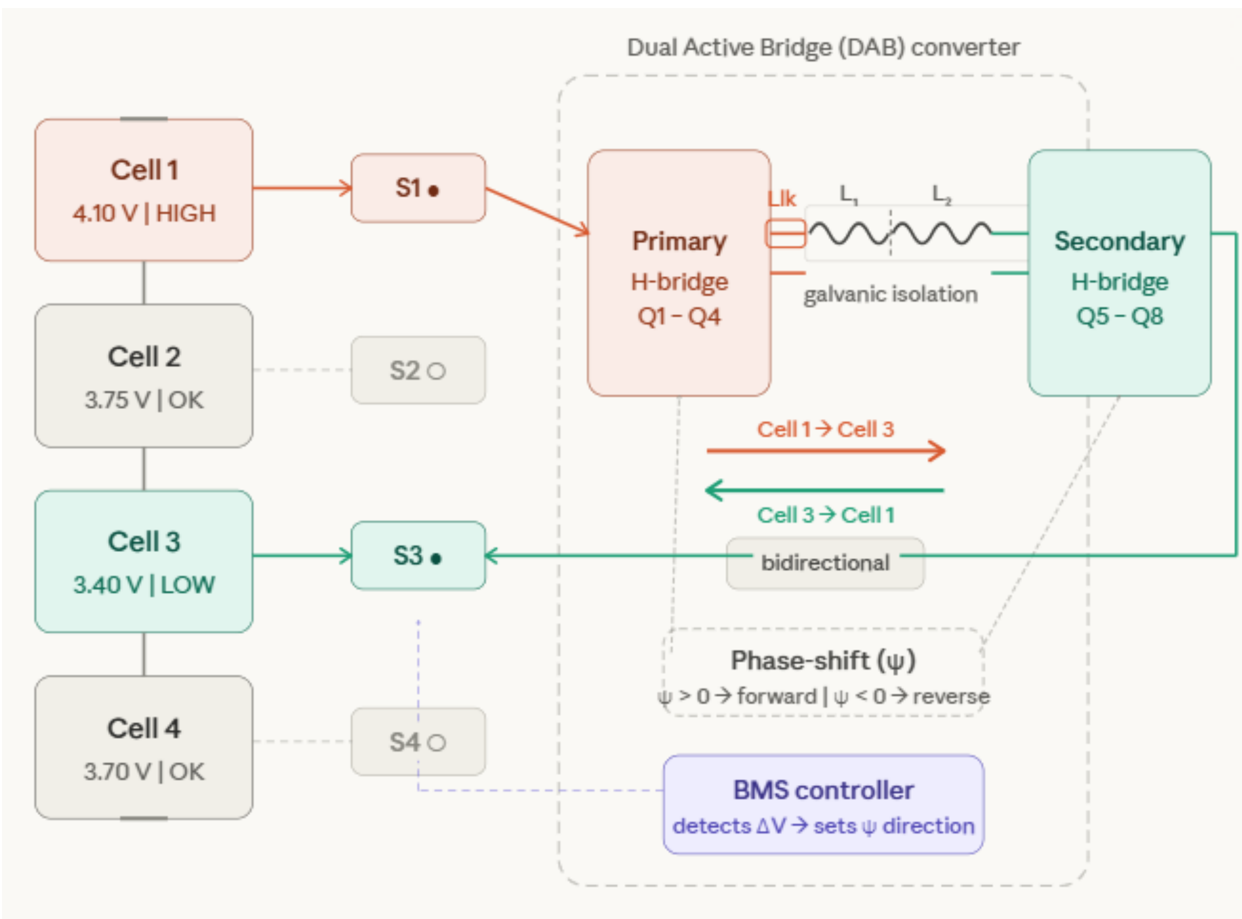

Figure 5 illustrates the complete cell-to-cell balancing scenario enabled by DAB's bidirectional architecture. The BMS operates as an intelligent energy router: when it identifies Cell 1 as the highest-voltage source (4.10 V) and Cell 3 as the lowest-voltage target (3.40 V), it closes switches S1 and S3, connecting Cell 1 to the primary H-bridge and Cell 3 to the secondary H-bridge. The system then initiates a direct energy transfer, pumping charge from the overcharged Cell 1 to the undercharged Cell 3.

The direction of energy flow is governed entirely by the sign of the phase-shift angle ψ. When $\psi > 0$, the primary bridge leads and power flows from Cell 1 to Cell 3. When $\psi < 0$, the secondary bridge leads and the flow reverses, delivering energy from Cell 3 back toward Cell 1 if conditions require. When $\psi = 0$, the bridges are synchronized, and no power is transferred. This precise manipulation of bridge timing allows the BMS controller to switch balancing direction instantaneously based on real-time voltage monitoring, with no hardware reconfiguration required.

This method offers far greater efficiency than traditional bucket brigade capacitive balancers, which move energy step by step through intermediate storage elements. In contrast, the DAB transfers charge directly between the source and destination cells, routinely achieving efficiencies above 90% (Li et al. 2025; Zhao et al. 2023). The architecture is inherently scalable, making it well suited for both cell to cell and module to module balancing in large battery systems.

Figure 6. DAB Converter Control Algorithm Flowchart

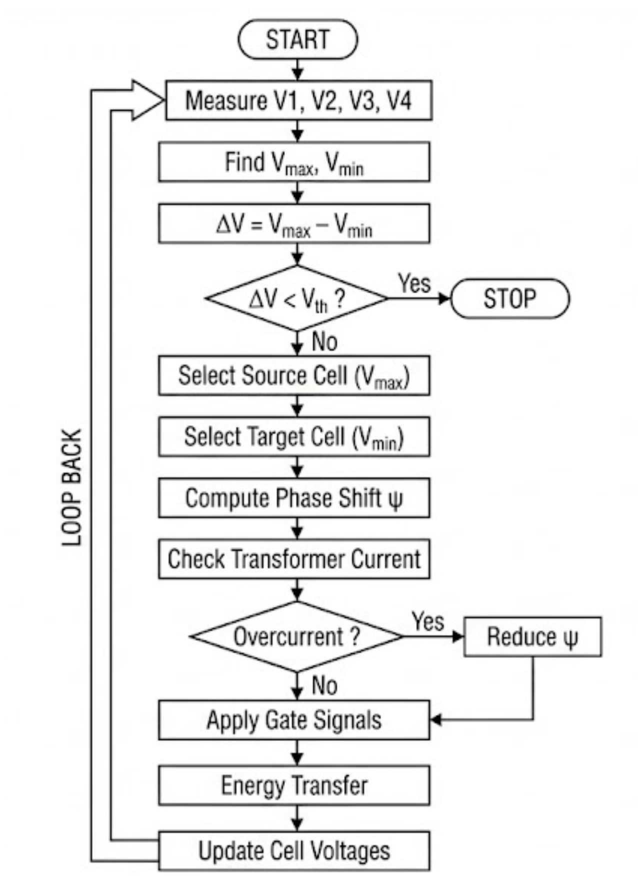

The complete control operational sequence of the DAB balancing system is shown in Figure 6. The control algorithm begins by measuring the individual voltages V_1, V_2, V_3, and V_4 of all cells in the series string. The controller then identifies the maximum and minimum values, V_{max} and V_{min}, and calculates the total voltage imbalance $\Delta V = V_{max} - V_{min}$. If ΔV falls below the predefined threshold V_{th}, typically set between 10 mV and 20 mV, the system determines that the pack is sufficiently balanced and halts operation. If the imbalance exceeds V_{th}, the algorithm proceeds to select the source cell carrying V_{max} and the target cell carrying V_{min}, then computes the required phase-shift angle ψ using the power transfer relationship (Muhammetoglu and Jamil 2024):

$$P = \frac{n \cdot V_{max} \cdot V_{min}}{2 \cdot f_{s} \cdot L_{lk}} D(1 - D) \qquad (1)$$

Here the variables are defined as follows:

- D = ψ/ω, the phase-shift ratio, with ω = 2πfs
- fs = switching frequency
- n = turns ratio of the transformer (primary: secondary)
- Vmax = maximum input or bus voltage
- Vmin = minimum input or bus voltage
- Llk = leakage inductance of the transformer, measured in Henries
- D = duty cycle, ranging from 0 to 1

Before applying the gate signals, the controller checks the transformer current $i_{tr}$for overcurrent conditions. If the current exceeds safe limits, the controller reduces ψ to throttle the power flow before proceeding. Once the current is confirmed within bounds, the gate signals are applied to the MOSFETs, energy transfer takes place, and the cell voltages are updated. The algorithm then loops back to remeasure all cell voltages and repeat the process until the pack reaches balance. This continuous loop ensures the system responds dynamically to changing conditions, maintains safety throughout operation, and maximizes the usable capacity and longevity of the battery pack.

A critical advantage of the DAB architecture over traditional flyback or buck–boost converters is its inherent ability to achieve zero-voltage switching (ZVS). By leveraging energy stored in the transformer's leakage inductance, the power switches transition states with minimal voltage across them, reducing switching losses and thermal stress. This enables practical high-frequency operation with smaller, lighter magnetic components and without excessive heat generation.

2.4 Summary of Active Cell Balancing Topologies

Having examined the working principles, advantages, and disadvantages of each topology in detail, **Table 1** summarizes the three primary active cell balancing approaches across four core dimensions: component type, advantages, disadvantages, and target applications.

- **Capacitor-based systems** are the most straightforward and cost-effective, utilizing a simple structure that requires no complex voltage sensing or closed-loop control. However, they suffer from slow balancing speeds and lose efficiency as cell voltage differences decrease, making them best suited for small-scale applications.

- **Inductor-based balancing** offers a more compact and adaptable design that can interface with various state of charge (SoC) control schemes. Its main limitations include sequential energy transfer and magnetization losses that increase overall balancing time as the number of cells grows.

- **DC/DC converter-based systems**, specifically those with embedded transformers, represent the high-end solution. They provide high accuracy, bidirectional flow, and crucial galvanic isolation for safety-critical tasks. While they are the most flexible and intelligent of the three, they carry significant trade-offs in terms of cost, physical bulk, and increased electromagnetic interference (EMI) stemming from their complex switching circuitry (Ashraf et al. 2025; Li et al. 2025; Zhao et al. 2023).

Table 1. Performance Benchmark and EV Application Suitability of Active Cell Balancing Topologies

Components of energy transfer	Advantages	Disadvantages	Applications
Capacitor-based	Simple structure; low cost; no voltage sensing or closed-loop control required.	Low balancing speed; efficiency drops with small voltage differences.	Small-scale systems with low accuracy and speed requirements.
Inductor-based	Compact design; fewer components; adaptable to various SoC control schemes.	Balancing time increases with more cells; magnetization loss; sequential energy transfer.	Medium-scale packs requiring moderate performance and simple design.
DC/DC converter based (transformer-embedded)	Supports galvanic isolation and high energy transfer accuracy; suitable for bidirectional flow and flexible control strategies.	Large physical size; high cost; complex control; possible EMI concerns.	High-voltage or safety-critical applications needing isolation; advanced battery systems requiring flexible, high-speed balancing.

3. Active Cell Balancing Analysis

The section 3 presents simulation-based analysis of inductor-based and DAB converter-based cell balancing, conducted using the MATLAB/Simulink platform (MathWorks 2024). Consequently, driven by the efficiency limitations inherent in capacitor-based schemes and the growing industry preference for robust, high-current solutions, this study specifically designs and analyzes inductor-based and DAB-based active cell balancing architectures. It is important to acknowledge the boundary conditions under which the following simulation results should be interpreted. The MATLAB/Simulink models presented in Sections 3.1 and 3.2 operate under idealized electrochemical assumptions: each cell is initialized with a uniform internal resistance and a fixed nominal capacity, and the simulated environment does not account for the cell-to-cell variability in resistance and capacity that accumulates in real battery packs through manufacturing tolerances, non-uniform thermal gradients, and electrochemical aging. These are not incidental omissions but deliberate constraints that define the simulation's role within this study—namely, to isolate and compare the intrinsic control-theoretic performance of each balancing topology under controlled, reproducible conditions. By holding cell parameters constant across topologies, the simulation provides a clean performance benchmark: differences in SOC convergence speed, voltage stability, and equalization efficiency in the results of Sections 3.1 and 3.2 can be attributed directly to topology architecture and control logic rather than to confounding variability in cell condition. This isolation is precisely what makes the hardware testing in Section 4 a necessary and complementary next step rather than a redundant one. Real lithium-ion cells exhibit state-dependent internal resistance, capacity fade as a function of cycle count, and self-discharge rates that diverge measurably between cells of the same nominal specification—none of which can be faithfully reproduced by idealized simulation alone. The empirical protocol in Section 4 is therefore designed to expose the balancing algorithms to exactly these real-world boundary conditions: intentionally imbalanced cell groups assembled from screened populations of good and degraded cells, tested under controlled charge–discharge cycling. Where simulations establish what each topology should achieve under ideal conditions, the hardware trials will determine how much of that theoretical performance survives contact with physical cell chemistry. Together, the two stages constitute a coherent research design in which simulation-derived hypotheses are subjected to empirical falsification—a structure that is standard in applied power electronics research and that positions the preliminary hardware results reported in Section 4 as the first stage of a validation pipeline rather than an afterthought.

Within these controlled boundary conditions, the simulation models make two deliberate algorithmic design choices that are worth making explicit, as they reflect engineering priorities that extend beyond the simulation environment to real-world BMS implementation. First, the two-cell control function (Appendix A) implements a 0.5% SOC tolerance threshold before any switching action is triggered. This deadband is not a simplification for convenience but an intentional design decision: without a minimum threshold, a control loop that compares two continuously evolving SOC values would trigger switch transitions at arbitrarily small differences, producing high-frequency gate oscillations that induce switching losses, electromagnetic interference, and accelerated thermal stress on the power electronics. The 0.5% tolerance window suppresses this chattering behavior and ensures that switching energy is expended only when meaningful charge redistribution is achievable. Second, the four-cell function (Appendix A) implements a tighter 0.2% deadband applied globally across the pack: once the spread between the maximum and minimum SOC falls below this threshold, all switching ceases entirely. This condition represents the practical definition of "balanced" in a production control context, where the cost of continued switching—in terms of power dissipation, component wear, and MCU processing overhead—exceeds the marginal benefit of further equalization at sub-0.2% differentials. Together, these two threshold parameters reflect a control philosophy oriented towards energy-efficient, hardware-safe operation rather than idealized mathematical convergence to zero error—a distinction that is consequential for the practical deployment of BMS algorithms in embedded automotive systems where processing bandwidth and component longevity are constrained.

3.1 Inductor-Based Cell Balancing Analysis

Figure 7 shows an inductor-based active cell balancing topology designed to enhance energy efficiency and prolong battery pack longevity. The system architecture, modeled in MATLAB/Simulink (MathWorks 2024) as depicted in Figure 7, utilizes a central inductor as an intermediate energy storage element to transfer charge between cells, thereby minimizing the thermal losses associated with passive resistive balancing. The control logic relies on a continuous monitoring algorithm that inputs the state of charge (SOC) for multiple cells alongside a pulse width modulation (PWM) signal. The algorithm computes the minimum SOC value across the pack and iteratively compares it against individual cell voltages (e.g., SOC1, SOC2) to identify the most depleted unit. Upon detection, the controller triggers the specific semiconductor switches associated with that branch, effectively directing energy to the lowest-charged cell until equalization is achieved.

Figure 7. Inductor-Based Cell Balancing with Two Cells

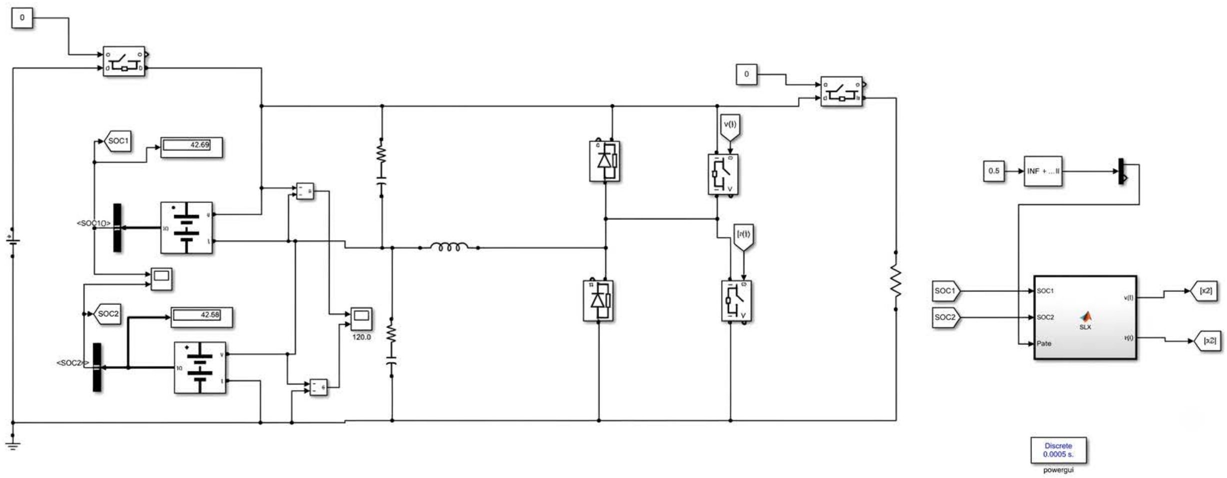

To validate the active balancing method, the simulation utilizes a lithium-ion battery model configured with specific electrical characteristics typical of high-energy-density applications. As detailed in the parameter configuration (Figure 8), each cell is defined with a nominal voltage of 3.7 V and a rated capacity of 5.4 Ah. The simulation is initialized with the batteries at a 50% state of charge, allowing for the observation of both charging and discharging balancing dynamics. Additionally, the model incorporates a battery response time of 15 seconds, ensuring that the transient voltage behaviors and chemical reaction delays are accounted for during the active balancing intervals. These parameters ensure the simulation results closely mirror the behavior of physical Li-ion cells under load.

Figure 8. Battery Parameters

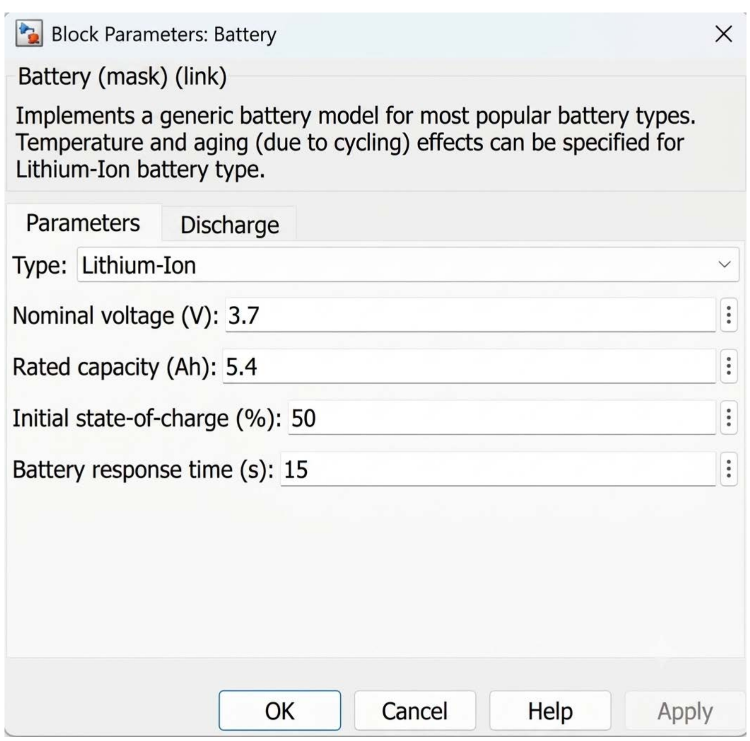

Figure 9. SOC Variations Over 30 Seconds

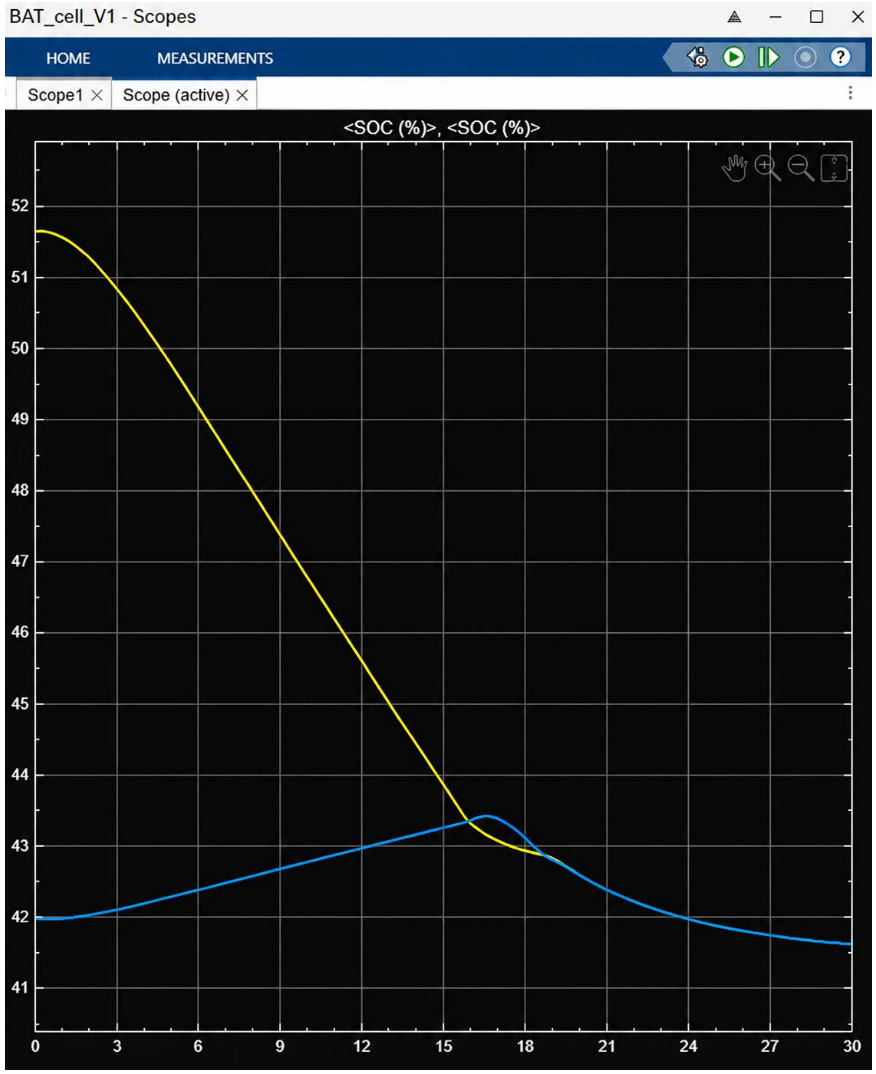

In Figure 9, the effectiveness of the balancing algorithm is visualized in the scope output. The plot tracks the SOC percentages of the two cells over a 30-second simulation period. Initially, the two cells exhibit a significant disparity in their charge levels: one cell starts at approximately 51.6% (yellow trace) while the other is near 42% (blue trace). As the active balancing mechanism operates, energy is transferred from the higher-charged cell to the lower-charged one. This is evidenced by the rapid decline of the yellow curve and the simultaneous gradual rise of the blue curve. The two curves intersect and converge at approximately the 18-second mark, settling at a unified SOC of roughly 43%. This convergence demonstrates the system's ability to successfully equalize the cell charges within a relatively short timeframe.

Figure 10. Cell Voltage Variations Over 30 Seconds

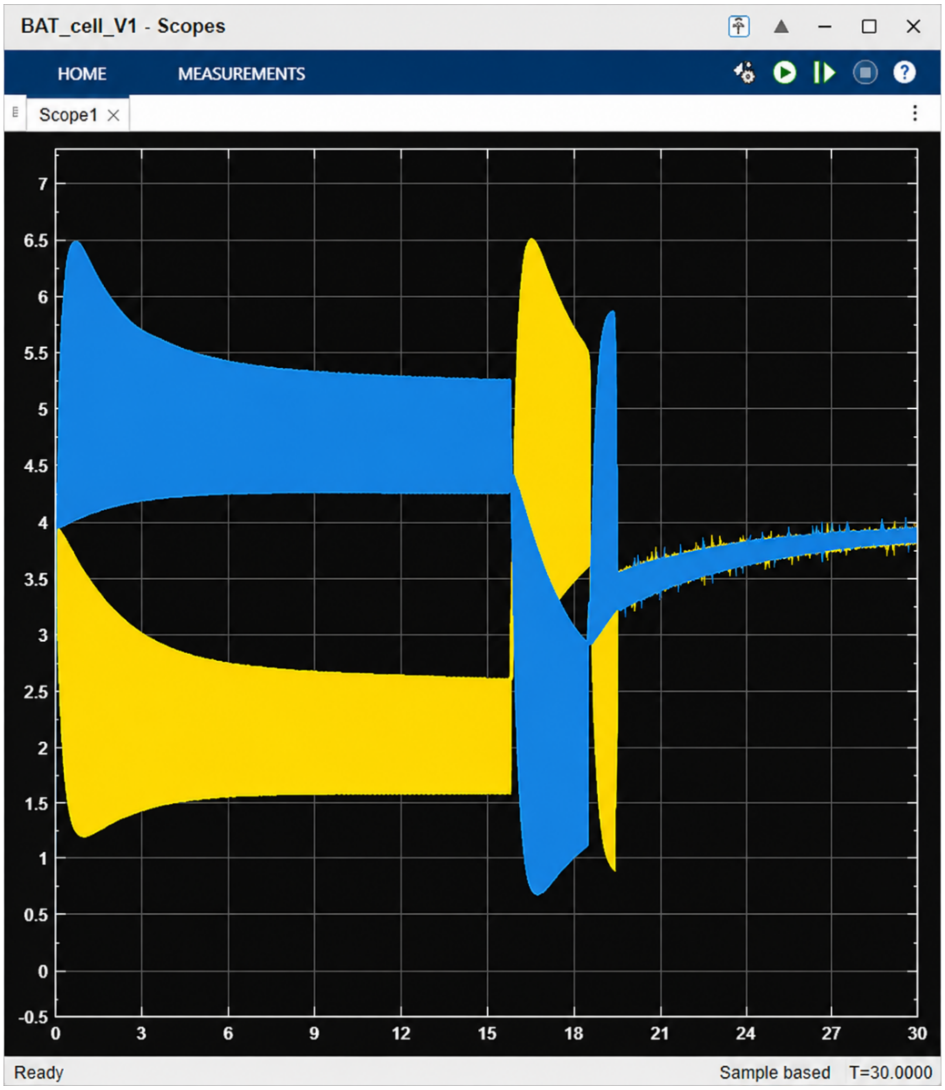

Figure 10 illustrates the instantaneous voltage variations across the two battery cells over a 30-second simulation interval. During the initial phase (0 to approximately 18 seconds), the graph reveals significant high-frequency oscillations in both voltage waveforms (yellow and blue traces). These large amplitude ripples—ranging roughly between 1.5 V and 6.5 V—are characteristic of inductor-based active balancing circuits, where high-speed switching is employed to energize the inductor and transfer charge between cells. The distinct separation between the blue and yellow envelopes during this period indicates the active "push-pull" operation of the circuit as it moves energy from the higher-voltage cell to the lower-voltage one.

The voltage behavior in Figure 10 correlates directly with the SOC convergence observed in the previous scope results in Figure 9. Around the 18-second mark, a distinct transition occurs in Figure 10: the high-magnitude switching oscillations cease abruptly, and the two voltage waveforms converge. This point of stabilization aligns precisely with the moment the SOC curves intersect (as seen in the SOC scope), indicating that the control algorithm has successfully detected that the cells are balanced (SOC1 = SOC2). Consequently, the controller disables or reduces the PWM switching duty cycle to halt further energy transfer.

Following the equalization event (from 18 seconds to 30 seconds) in Figure 10, the system enters a steady state. The voltage traces for both cells stabilize into a narrow band, hovering near the nominal voltage level (approximately 3.5 V to 4 V) with minimal noise. This contrasts sharply with the chaotic transient response observed in the first half of the simulation. The eventual overlap of the blue and yellow lines in this final phase confirms that the cells have reached voltage equilibrium, validating the effectiveness of the inductor-based topology in achieving and maintaining a balanced state after the active cycle concludes. Based on the flowchart presented in Figure 11, the control logic designed for the two-cell balancing system can be described as follows. The routine begins by reading the current status inputs: SOC1, SOC2, and the system's PWM signal.

Figure 11. Flowchart for Inductor-Based Cell Balancing with Two Cells

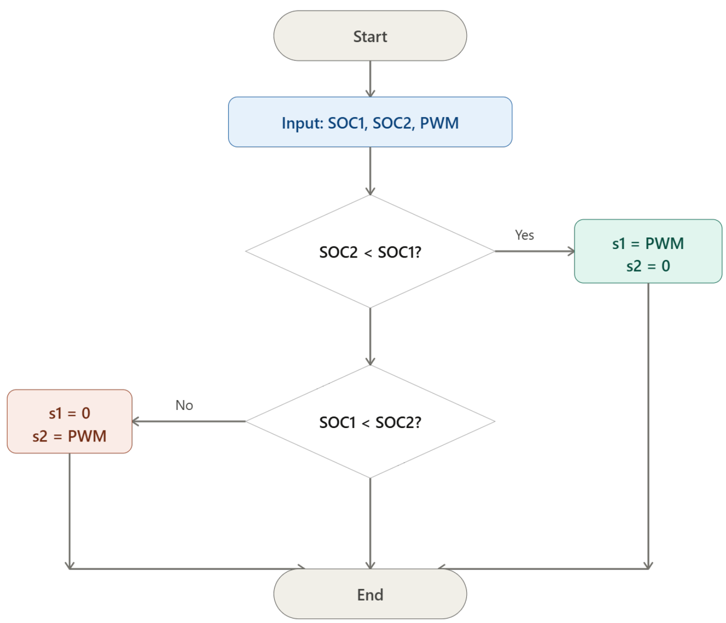

The algorithm then enters a primary decision block that compares the two charge levels, specifically checking whether SOC2 < SOC1. If this condition is satisfied—indicating that Cell 1 carries a higher charge—the system follows the "Yes" branch and executes an active balancing operation, setting output for the switch S1 to the PWM signal while holding the switch S2 at 0, thereby triggering the discharge of Cell 1 to transfer energy to the remainder of the circuit.

If the first condition is not met, the logic proceeds to a secondary conditional check to determine whether SOC1 < SOC2. This stage handles the scenario in which Cell 2 may be the higher-charged unit. The flowchart indicates a branching path that triggers the alternative action: setting S1 to 0 and assigning the PWM signal to S2, thereby activating the switch associated with Cell 2 to discharge and equalize with Cell 1. If neither balancing condition requires action, the flow converges to the “End” node, completing the control cycle.

Figure 12 presents an advanced inductor-based balancing circuit, scaled to accommodate a four-cell battery pack. Unlike the simpler two-cell model, this configuration integrates four distinct battery modules arranged in a series-parallel structure. Each battery block is equipped with individual voltage and SOC sensors to provide granular monitoring of the entire pack’s performance. Circuit complexity is increased significantly by the inclusion of multiple inductors—visible as the coiled components connecting the horizontal rails—which serve as the primary energy storage mediums for transferring charge between adjacent and non-adjacent cells. To manage energy flow across this larger array, the system employs a comprehensive network of power electronic switches (IGBTs/MOSFETs) distributed throughout the circuit branches, strategically placed to create selectable current paths. This modular design implies a sophisticated control strategy whereby the central controller can target any specific cell for equalization without disrupting the operation of intermediate cells.

Figure 12. Inductor-Based Cell Balancing with Four Cells

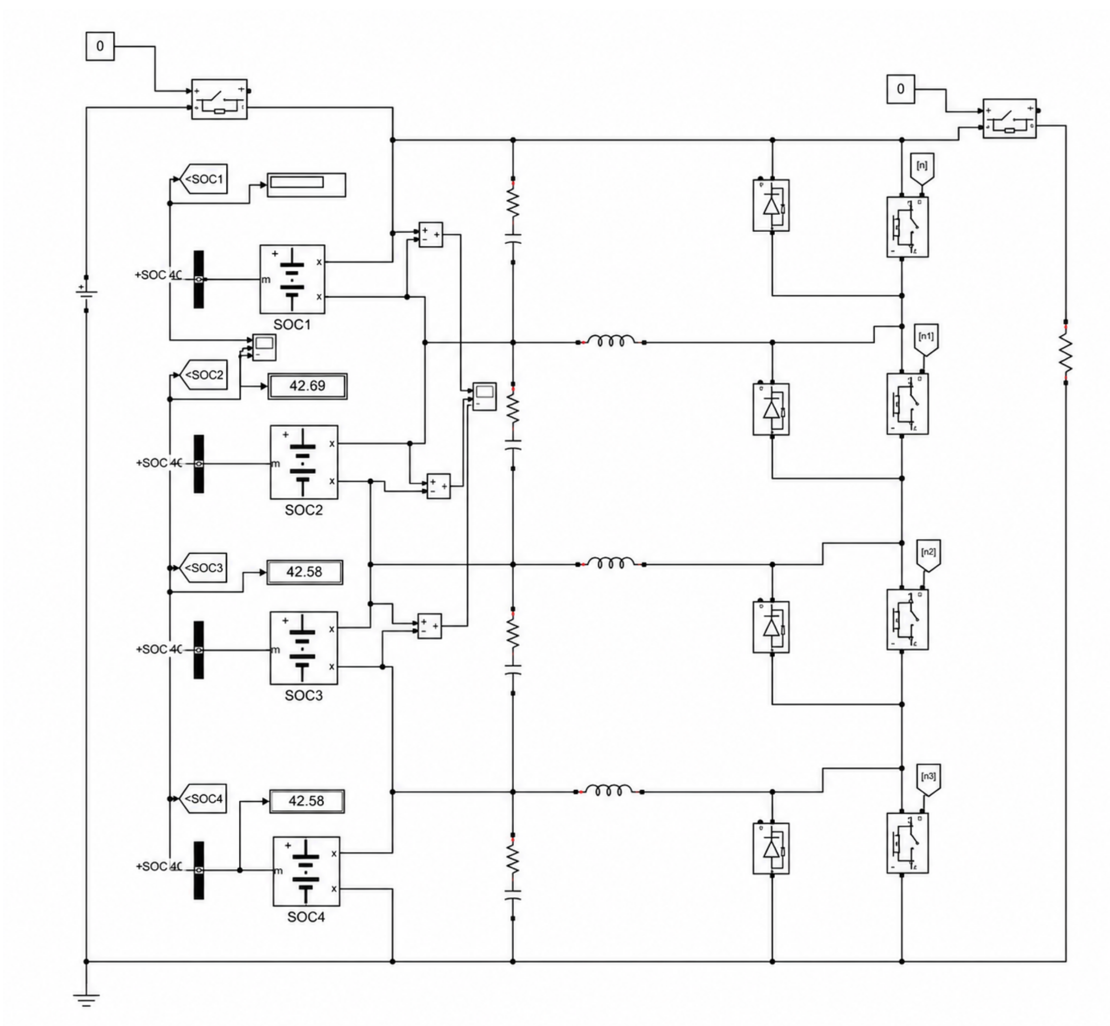

The control logic for the four-cell inductor-based balancing system follows a structured algorithmic sequence to ensure efficient energy redistribution. As depicted in Figure 13, the process begins by initializing monitoring parameters, specifically inputting the SOC values for all four battery cells (SOC1–SOC4) along with the PWM signal. The algorithm immediately proceeds to identify the lowest charge level present in the battery pack. Following this assessment, the system initializes the switch control variables (s1 through s4) to a default state of zero, ensuring no active balancing occurs until specific logic conditions are met.

The core decision-making process involves a conditional check to determine how many SOC values equal the minimum SOC identified in the preceding step. If a matching cell is identified, the algorithm follows the active balancing path, assigning the PWM signal to the corresponding switch variable (sX = PWM) to activate the charging circuit for the depleted cell. Conversely, if no condition is met, the system defaults all switches to zero to prevent current flow. The process concludes by outputting the final switch states to the hardware drivers, ready for the subsequent real-time control cycle.

Figure 13. Flowchart for Inductor-Based Cell Balancing with Four Cells

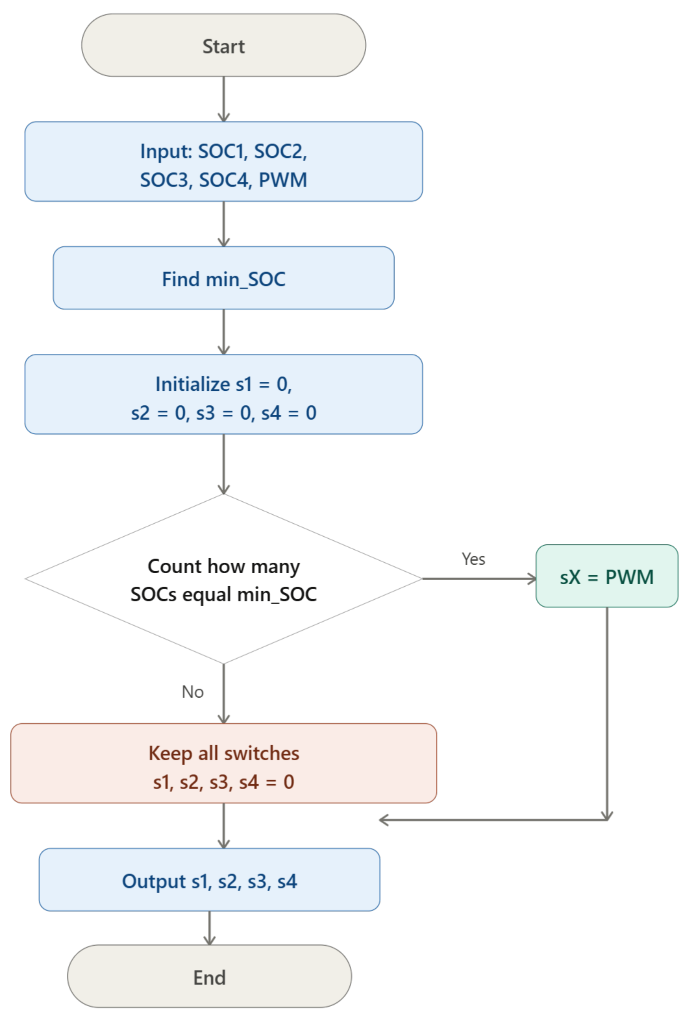

Figure 14 illustrates the state-of-charge (SOC) trajectories for four battery cells over an approximately 80-second simulation period under the inductor-based active balancing system. At the commencement of the balancing cycle (t = 0 seconds), the battery pack exhibits a substantial charge imbalance across the four cells: SOC2 (orange trace) starts at the highest level of approximately 89%, followed by SOC3 (yellow trace) at roughly 62%, SOC1 (blue trace) at approximately 47%, and SOC4 (purple trace) at the lowest initial value of around 23%. This initial spread of approximately 66 percentage points represents a severe imbalance scenario designed to rigorously test the DAB-based control algorithm.

As the simulation progresses, the balancing mechanism drives all four cells toward a common equilibrium. SOC4 (purple), starting from the lowest point, rises steeply as it receives energy from the higher-charged cells. SOC2 (orange) declines gradually from its peak of ~89%, while SOC3 (yellow) and SOC1 (blue) remain relatively stable in the early phase before beginning to converge. SOC1 and SOC3 merge first at approximately t = 12 seconds at around 47–48%, after which their combined trace continues to rise as energy redistribution proceeds. SOC4 steadily catches up throughout the mid-simulation period.

Full equalization of all four traces is achieved at approximately t = 60 seconds, where all cells converge at a common SOC of approximately 72%. Beyond this point, all four traces overlap and remain stable at this unified level for the remainder of the simulation, confirming that the balancing algorithm has successfully brought the pack to equilibrium. This result demonstrates the high effectiveness of the DAB-based topology in handling large initial imbalances and achieving rapid, stable cell equalization.

Figure 14. SOCs Variations in the Inductor-Based Cell Balancing with Four Cells

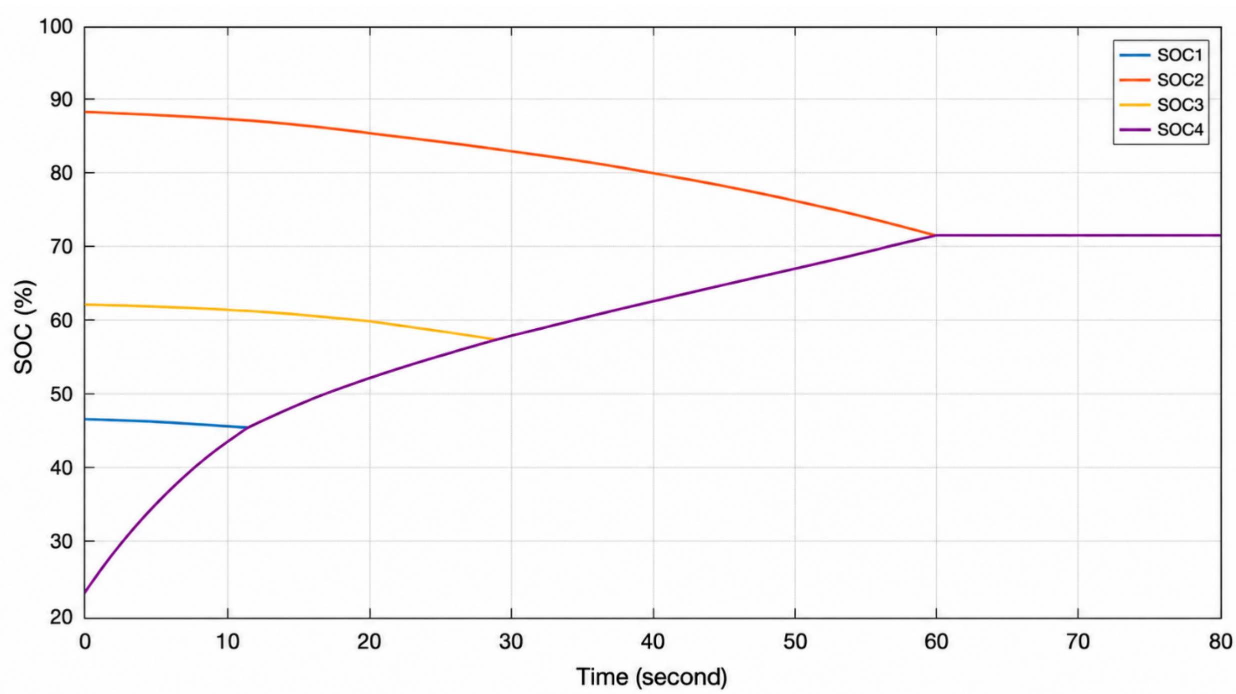

3.2 DC-to-DC Converter-Based Cell Balancing Analysis

Figure 15. DAB Converter MATLAB/Simulink Model

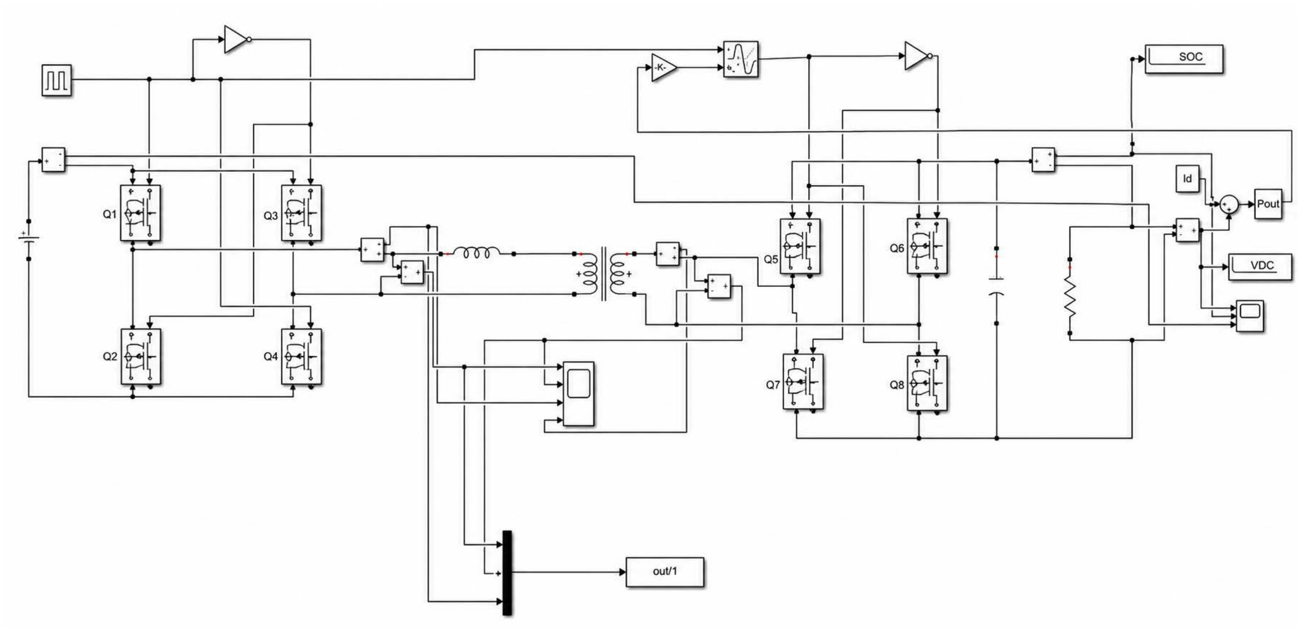

Figure 15 illustrates the MATLAB/Simulink (MathWorks 2024) implementation of a DAB DC-to-DC converter—a topology distinct from the previously discussed cell balancing circuits.

The model is equipped with measurement blocks to monitor system performance in real time. Digital displays in the simulation window indicate instantaneous values, with one output voltage reading approximately 48.08V in Figure 15, likely representing the regulated output voltage across the load. The secondary side also includes a capacitor placed in parallel with the resistive load to filter voltage ripples and ensure a stable DC output. The presence of scopes and product blocks indicates that the simulation is configured to analyze power efficiency and transient response characteristics.

Figure 16 presents the steady-state voltage and current characteristics of the DAB converter over multiple switching cycles. The plot displays three critical system variables: the primary bridge voltage (V_p, shown in blue), the secondary bridge voltage (V_s, shown in orange), and the leakage inductor current (I_p, shown in pink). Both voltage signals exhibit clear high-frequency square-wave profiles, confirming the correct switching operation of the full-bridge inverters on both sides. A distinct voltage scaling is observable, with the primary side operating at a higher amplitude (approximately ±100 V) compared to the secondary side (approximately ±50 V), reflecting the transformer's turns ratio or the specific DC bus voltage levels defined in the simulation.

Figure 16. Waveforms in DAB Converter

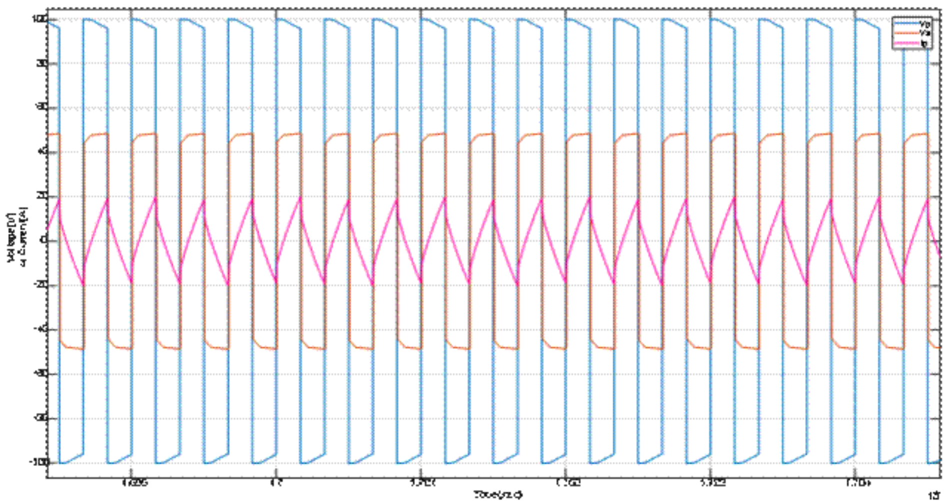

Figure 17 provides a zoomed-in perspective of the waveforms, enabling a detailed analysis of the PSM control strategy. This close-up view clearly reveals the temporal delay (phase shift) between the rising edges of the primary voltage (Vp) and the secondary voltage (Vs). In this specific operating scenario, the primary voltage leads the secondary voltage, dictating that power flow is directed from the primary source to the load. Additionally, the inductor current (Ip, pink trace) follows a piecewise linear, triangular trajectory consistent with inductive circuit laws (V = $L\frac{di}{dt}$), wherein the current slope is determined by the instantaneous voltage difference applied across the leakage inductance (Erickson and Maksimovic 2001).

The interaction between the voltage square waves and the inductor current demonstrates the converter's ZVS potential and power transfer capability. The active phase shift creates a voltage differential across the series inductor, forcing the current to ramp up or down to facilitate energy transfer between the DC domains. The stability of the peak current values and the uniformity of switching cycles in Figure 17 confirm that the control loop has successfully locked the phase angle to maintain constant output regulation, validating the robustness of the implemented control logic.

Figure 17. Zoomed Waveforms in DAB Converter

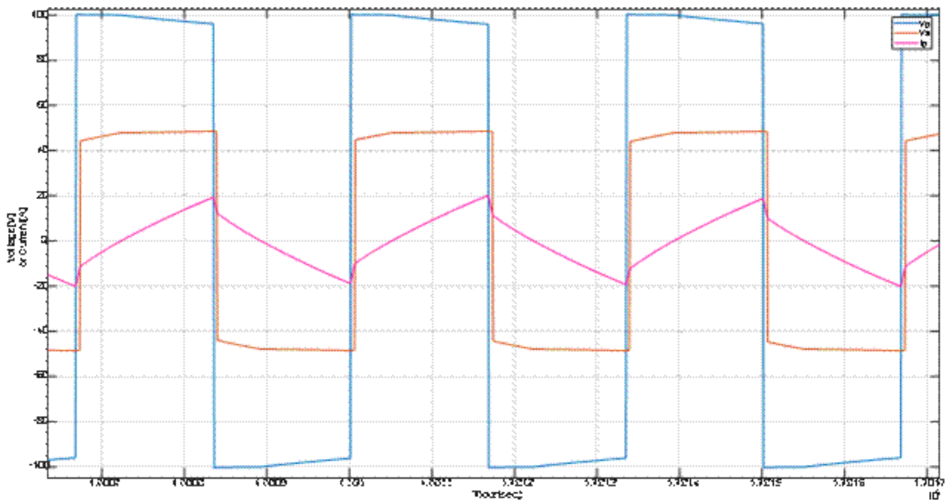

Figure 18. MATLAB/Simulink Schematic Based on DAB for Four-Cell Balancing

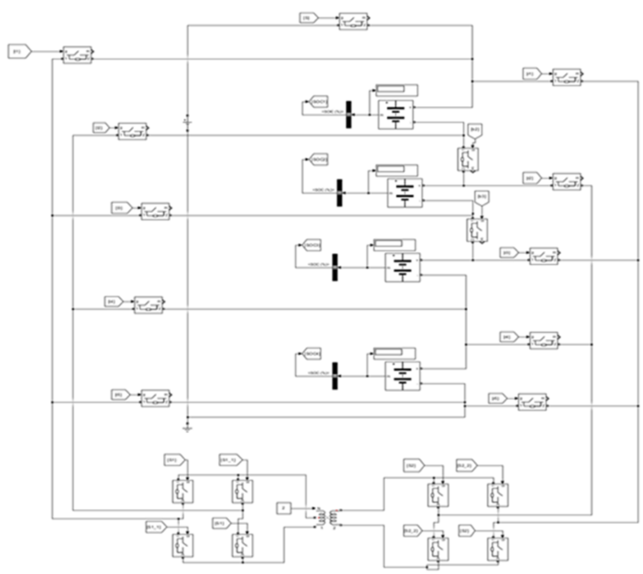

Figure 18 shows a Dual Active Bridge (DAB) converter MATLAB/Simulink schematic for balancing four battery cells.

The flowchart in Figure 19 illustrates the control algorithm that selects the battery cell with the lowest SOC among four cells and applies the corresponding control settings in the DAB converter. The process begins by reading SOC1–SOC4 along with a PWM input, computing a vector of SOC values, and determining the minimum SOC (SOC_{min}). The algorithm then compares SOC1 through SOC4 sequentially against SOC_{min}, and upon finding a match, activates the branch settings associated with that specific cell. This structured decision flow ensures that the cell with the lowest charge is consistently identified and prioritized for balancing action.

Figure 19. Flowchart for the Control Algorithm for Four-Cell Balancing

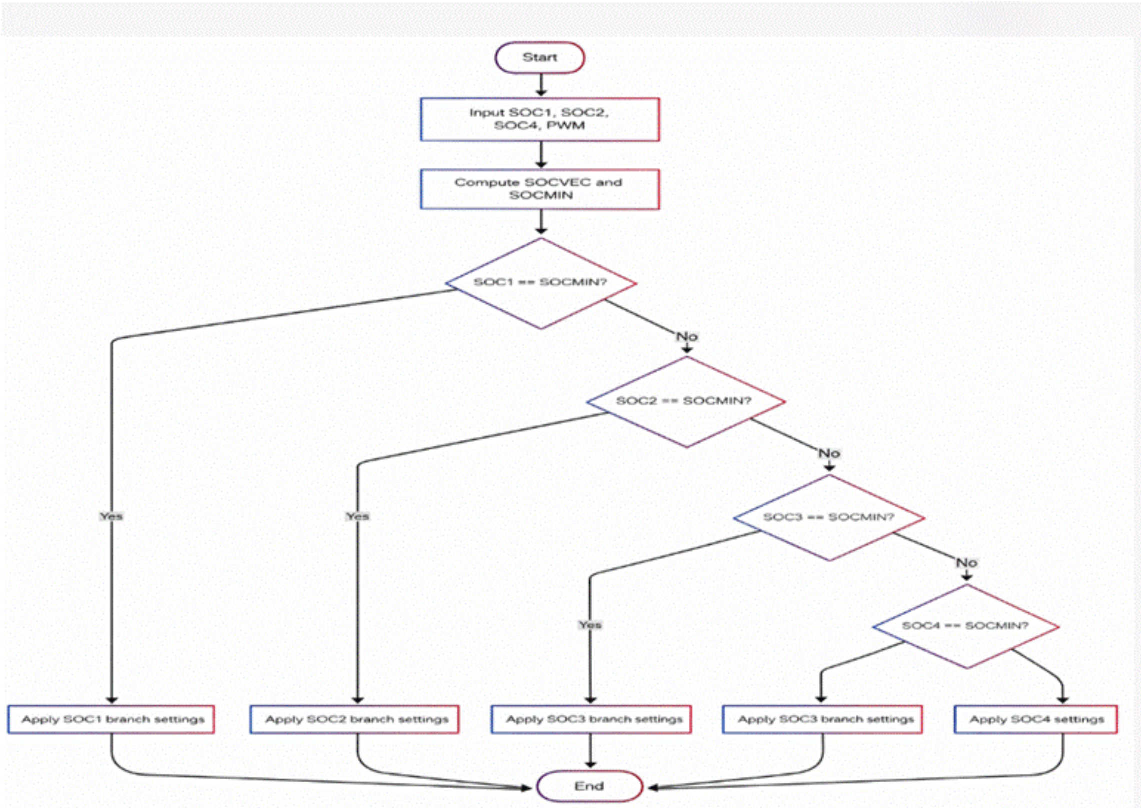

Figure 20 illustrates the state-of-charge (SOC) trajectories for four battery cells over a 120-second simulation period under the inductor-based active balancing system. At the commencement of the balancing cycle (t = 0 seconds), the battery pack exhibits a clear charge imbalance across the four cells: SOC1 (blue trace) starts at the highest level of approximately 60%, followed by SOC2 (red/orange trace) at roughly 49%, SOC3 (yellow trace) at approximately 40%, and SOC4 (purple trace) at the lowest initial value of around 30%. This initial spread of approximately 30 percentage points constitutes a significant imbalance scenario designed to test the effectiveness of the control algorithm.

As the simulation progresses, the balancing mechanism acts rapidly on SOC2, SOC3, and SOC4. SOC2 and SOC3 decline steeply from their initial values, while SOC4 rises slightly from its lowest point as it receives redistributed energy. All three traces converge at approximately t = 25 seconds at a common value of roughly 35%, confirming that the controller successfully identifies and targets the higher-charged cells for discharge toward the pack's minimum baseline.

SOC1, carrying the largest initial charge surplus at 60%, continues to decline at a comparatively slower but steady rate throughout the remainder of the simulation. It gradually approaches the converged group, finally merging with the other three traces at approximately t = 100–105 seconds at around 35–36%. Beyond this point, all four traces overlap and remain stable at approximately 35–36% for the remainder of the 120-second timeline.

This prolonged but ultimately successful equalization confirms that the inductor-based algorithm correctly prioritizes the most imbalanced cells first, handling the largest charge differential (SOC1) last. The result validates both the accuracy of the control logic and the scalability of the topology in managing four cells with varying initial charge states.

Figure 20. SOC Variations in DAB Converter-Based Cell Balancing with Four Cells

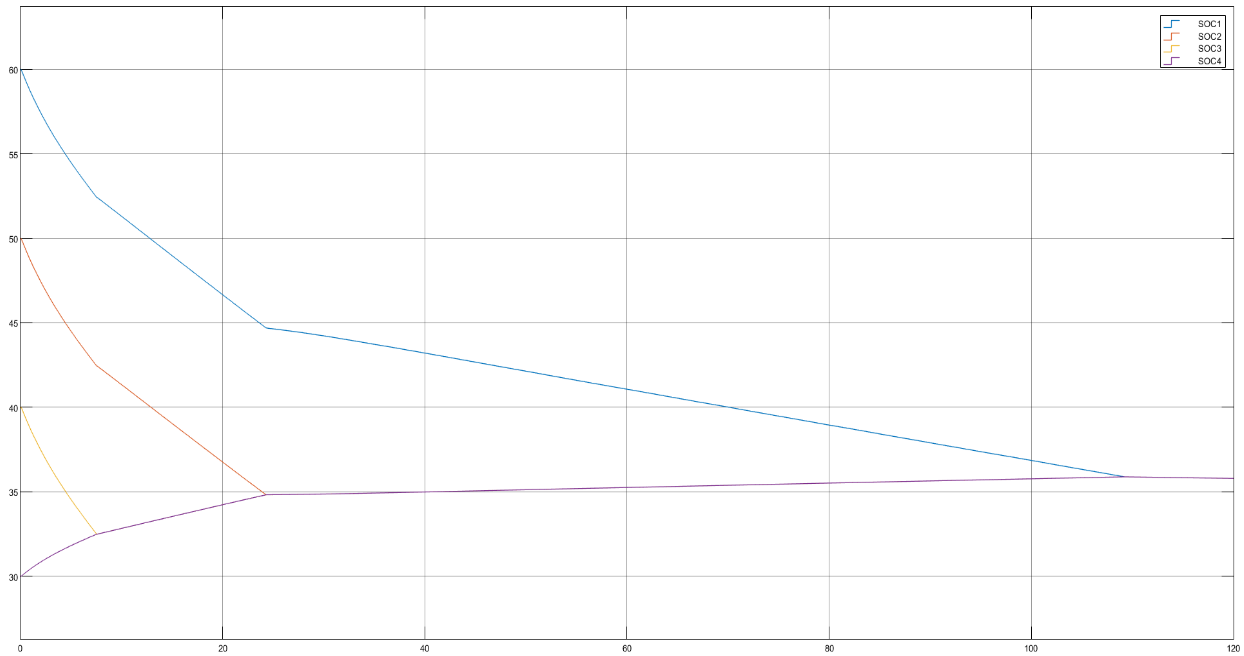

4. Battery Test

This section describes the ongoing empirical battery testing program, which is designed to validate the simulation findings presented in Section 3 under real-world cell chemistry conditions. The testing is currently in progress; the methodology and preliminary results are reported here, and full topology-by-topology comparison results will be presented in future work.

The motivation for this testing phase is straightforward: the MATLAB/Simulink models in Section 3 operate under idealized assumptions of uniform internal resistance and cell capacity. Physical cells exhibit state-dependent resistance, capacity fade, and self-discharge rates that diverge between cells of the same nominal specification. The empirical protocol described below is designed to expose the balancing algorithms to exactly these conditions—intentionally imbalanced cell groups constructed from screened populations of good and degraded cells—to determine how much of the theoretical performance from Section 3 survives contact with physical battery chemistry.

4.1 Impact of Cell Balancing

Battery cell balancing plays a very critical role in determining the efficiency, durability and sustainability of current modern EVs (Omariba, Zhang, and Sun 2019). Current EV battery packs typically consist of hundreds of Li-ion cells connected in series and parallel configurations to collectively meet EV voltage and energy requirements (Yildirim et al. 2019). Due to inevitable manufacturing variability, aging effects, and non-uniform thermal conditions, individual cells within a pack gradually diverge in capacity, internal resistance, and self-discharge behavior. Without effective cell balancing on EV, these inconsistencies will accumulate over time and could lead to reduced usable energy, increased energy losses, accelerated degradation, and higher operational and environmental costs (Qi and Lu 2014). Good cell balancing is not only an important technique for EV module/pack control, but also a system-level enabler for more efficient electrified transportation. Specifically, cell balancing typically has several impacts that fall under the following five key categories:

Overall Energy Consumption

One of the direct impacts of cell balancing is the reduction of overall energy consumption during EV operation (Safari et al. 2025). In a series-connected battery string, the total usable energy of the entire pack is usually constrained by the weakest cells, as charging and discharging must terminate when any single cell reaches its voltage limits. In the absence of proper balancing, cell-to-cell SOC divergence could cause early cutoffs and leave substantial residual energy unused in healthier cells.

Cell balancing could mitigate this issue by equalizing SOC among cells, thereby maximizing the accessible capacity of the battery pack during both charge and discharge. By improving pack utilization, balancing reduces the frequency and depth of charging events required to achieve a given driving range. This directly lowers the total electrical energy drawn from the grid over the vehicle's lifetime. Additionally, balancing reduces internal losses associated with uneven current distribution and excessive voltage polarization in weaker cells. Lower resistive losses translate into higher drivetrain efficiency, particularly during high-power operation such as acceleration and regenerative braking. As EV adoption increases quickly, even modest efficiency improvements on vehicles through effective cell balancing could lead to substantial cumulative energy savings at the fleet level (Lee, Drury, and Mellor 2011).

Stress on Current Electrical Grid Infrastructure

The rapid expansion of EV fleets places increasing demands on electrical grid infrastructure, particularly in urban areas where charging loads are spatially and temporally concentrated (Engel et al. 2018). Cell balancing contributes to grid resilience by reducing both peak and cumulative charging demand. Balanced battery packs maintain higher usable capacity and more predictable voltage behavior, allowing vehicles to operate longer between charging sessions. This reduces the frequency of charging events and smooths aggregate demand profiles.

Furthermore, effective balancing improves charge acceptance during fast charging by preventing early termination caused by overvoltage in a single cell. As a result, charging sessions become more energy-efficient and less prone to extended constant-voltage phases, which are associated with lower power transfer efficiency and longer grid connection times. On a system scale, balanced packs enable more efficient utilization of existing charging infrastructure and reduce the need for costly grid upgrades to accommodate rising EV penetration (Khalid et al. 2019). In this way, cell balancing indirectly supports the scalability of transportation electrification within the constraints of current power generation and distribution systems.

Battery Service Life and Degradation

Cell balancing significantly influences the long-term durability of EV battery packs (Adebowale 2025). Imbalance among cells accelerates degradation through multiple mechanisms, including repeated overcharge and over-discharge of specific cells, increased thermal stress, and uneven current sharing in parallel groups. These stressors disproportionately affect weaker cells, creating a positive feedback loop in which imbalance worsens with each cycle, ultimately leading to premature pack failure.

Balancing interrupts this feedback loop by preventing individual cells from operating outside their optimal SOC windows. By maintaining uniform SOC and voltage distribution, balancing reduces exposure to high-voltage stress at the upper end of charge and deep discharge stress at the lower end. This mitigation slows key degradation processes such as lithium plating, electrolyte oxidation, and impedance growth. Consequently, balanced packs exhibit slower capacity fade and reduced resistance increase over time, extending their service life. From a vehicle design perspective, improved battery life directly enhances reliability and reduces the likelihood of early battery replacement.

Life Cycle Cost Reduction

The extension of battery service life by effective cell balancing translates directly into lower lifecycle costs for EV users (Sultan et al. 2025). The battery pack is the most expensive component on EV, and its replacement is a significant financial burden for users. By preserving usable capacity and delaying end-of-life conditions, balancing reduces the cost of the battery over the vehicle's lifetime. In addition to reducing replacement frequency, balancing improves energy efficiency and usable range, lowering electricity consumption per kilometer driven. This results in reduced operating costs for vehicle owners as well. Balanced battery packs also exhibit more predictable performance, reducing the likelihood of unexpected range loss or sudden degradation that can lead to costly maintenance interventions. Over the full lifecycle of an EV, these benefits collectively improve the total cost of ownership, making EVs more economically attractive to consumers and accelerating market adoption.

Environmental Benefits and Sustainability

Cell balancing also contributes to environmental sustainability by reducing the material and energy footprint of EV batteries (Dunn et al., 2015). Extended battery life reduces the demand for new battery production, which is associated with energy-intensive manufacturing processes and the extraction of critical raw materials such as lithium, nickel, cobalt, and manganese. By maximizing the useful lifetime of existing batteries, balancing helps mitigate resource depletion and reduces upstream environmental impacts. Lower energy consumption during vehicle operation and charging further decreases indirect greenhouse gas emissions, particularly in regions where electricity generation relies partially on fossil fuels. Moreover, longer-lasting batteries improve the feasibility of second-life applications, such as stationary energy storage, by preserving sufficient capacity and uniformity at the end of automotive service. This enhances the circularity of battery usage and reduces waste generation. From a lifecycle assessment perspective, cell balancing plays an important role in improving the overall environmental performance of EV technology (Yang, Huang, and Lin 2022).

4.2 Experimental Setup

Preconditioning and Preparation of Battery Cells

Figure 21. Precondition and Single Cell Preparation

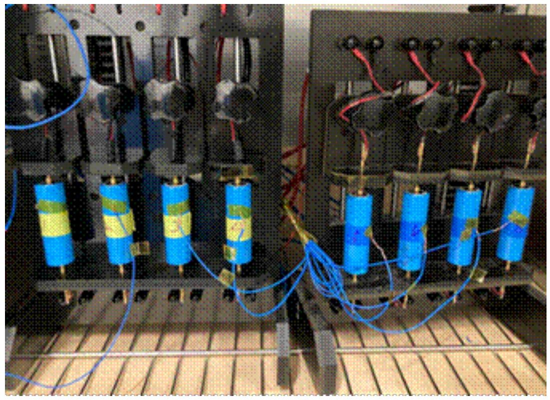

To minimize the influence of unknown prior usage and to establish repeatable baselines, each battery cell was preconditioned using two formation-like cycles at room temperature (25 °C) as shown in Figure 21. Each charging-discharging cycle consisted of a constant current–constant voltage (CC–CV) charge to 4.20 V, followed by a CV hold until the current tapered off. After a subsequent rest period, a CC discharge was applied down to 2.5 V, followed by a final rest period. For the charging phase, the CC rate was selected within the range of 0.3C–0.5C, and the CV hold was maintained at 4.20 V until the battery was fully charged. Rest periods of 30–60 minutes were implemented after both charging and discharging to allow the open-circuit voltage (OCV) to relax and stabilize. Following the preconditioning phase shown in Figure 21, a baseline capacity test was performed at a low rate to determine the initial capacity of the cells.

Self-Discharge Test (Single-Cell Screening for Degraded Cells)

A single-cell self-discharge test was used as the first screening step to identify cells with abnormal leakage or unusually fast OCV decay. Each cell was charged to a given voltage using the CC–CV method described above. After charging, the cell was held in an open circuit and allowed to rest for a defined observation window. During this rest period, cell voltage was recorded at regular intervals (e.g., every 10 minutes during the first hour and every 30 minutes thereafter) for a total of 3 hours as a minimum screening duration.

The self-discharge metric was quantified using the OCV drop from the end of the charge step to the end of the rest window, along with the slope of the voltage decay during later portions of the rest (to reduce the influence of immediate relaxation phenomena). Cells exhibiting an unusually large voltage drop relative to the population distribution were flagged as high self-discharge candidates and treated as “degraded” (or “abnormal”) for subsequent comparisons. This screening step enables intentional construction of imbalanced groups (good + degraded) in the later module-level tests. Figure 22 shows some of our self-discharging test results on EV NiMH cells (self-discharging of Li-ion cells are still under testing).

Figure 22. Self-Discharging Test Results on EV NiMH Cells

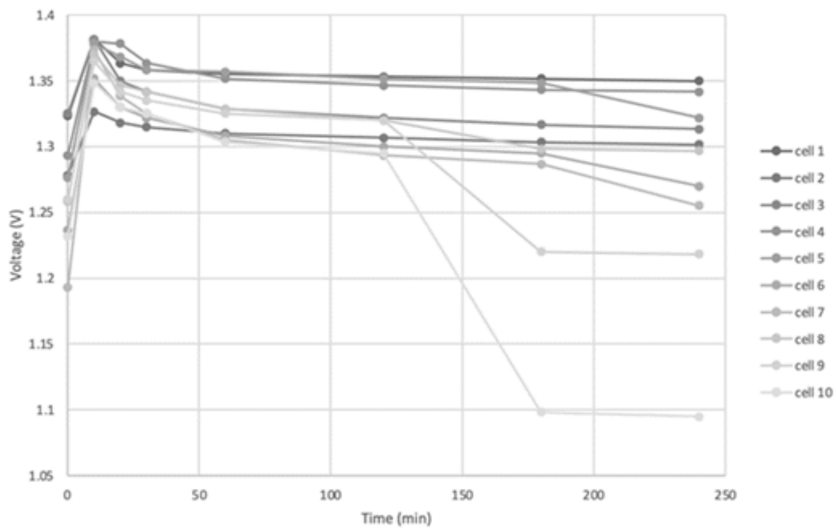

Standard Charge–Discharge Characterization and Impedance Test (Single Cell)

After screening, each cell underwent a controlled charge–discharge test to compare working voltage and usable capacity under consistent conditions. Cells were charged CC–CV to 4.20 V, rested for 30 minutes, and then discharged at a fixed current rate to 3V. A moderate rate such as 0.5C was typically used for characterization because it reveals polarization and resistance-related differences more clearly than a very low rate, while remaining within safe thermal limits for 18,650 cells. Impedance tests were also conducted on each battery cell as shown in Figure 23, which were repeated three times to ensure repeatability.

Figure 23. Cycling and Impedance Test on Single Li-ion Battery Cells : (a) Cycling Test; (b) Impedance Test

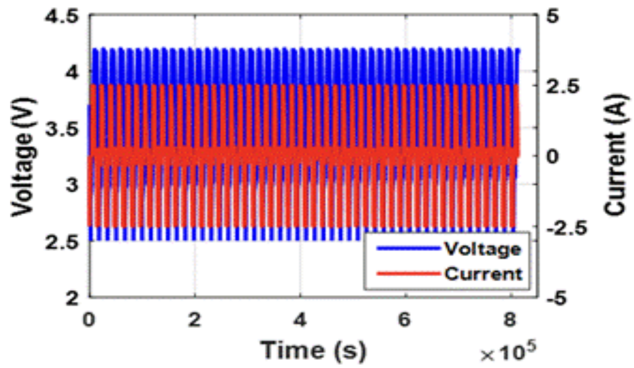

(a) Cycling Test

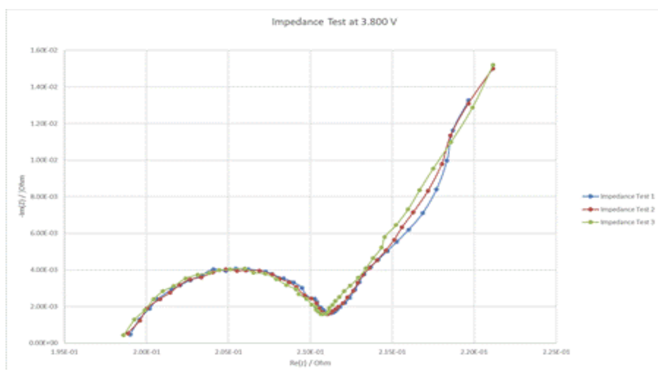

(b) Impedance Test

Rate-Performance Test (Single Cell)

Rate-performance behavior was conducted to quantify the dependence of accessible capacity and voltage stability on discharge current. The test consisted of multiple discharge steps conducted at increasing C-rates. For each step, the cell was first brought to a fully charged state, rested for 30–60 minutes, and then discharged to 3V at the selected C-rates. Such discharge rates included 0.2C, 0.5C, 0.8C, and 1C. For each discharge rate test, the cell was recharged fully using the same CC–CV method to maintain a consistent starting SOC. For each rate, the delivered discharge capacity (Ah), discharge energy (Wh), average voltage, and maximum temperature rise were recorded. Rate capability was reported as capacity retention relative to the baseline low-rate capacity. Cells with elevated internal resistance typically exhibited increased voltage sag and earlier cutoff, resulting in disproportionately reduced capacity at higher rates; these cells were prioritized for inclusion as “degraded” elements in mixed module configurations.

Group Configuration and Initial Equalization

To study the effects of imbalance, battery cells can be assembled into small modules using controlled configurations: series strings and series-parallel groups. Two categories of modules were constructed: balanced modules (all cells selected from the “good” population) and imbalanced modules (one or more cells intentionally selected from the “degraded” population identified via self-discharge and rate/capacity screening). This design enables direct attribution of module-level performance limitations to the presence of a known weak cell.

Before assembly, cells were equalized to a common voltage to prevent large inrush currents and uncontrolled balancing transients. For series strings, equalization was accomplished by charging each cell to a target state of charge (SOC) of 50% and resting until their open-circuit voltage (OCV) values were within ±5 mV of one another, in accordance with the laboratory's assembly protocol. For parallel groups, cells were brought to nearly identical open-circuit voltages before connecting in parallel to mitigate rapid, unmanaged equalization currents across the busbars. Following physical assembly, the module was allowed to rest for at least 60 minutes to ensure adequate voltage relaxation, after which each individual cell voltage was confirmed via the integrated cell taps.

Group Self-Discharge Test

To examine how imbalance manifests during rest, each module underwent an open-circuit storage test after a full charge. The module was charged fully, rested for 60 minutes, and then left under open circuit for an extended period. Group voltage and individual cell voltages were recorded periodically. The key observation was the evolution of cell-to-cell voltage spread during rest. Modules containing high self-discharge cells typically showed increasing divergence over time, with the degraded cell’s voltage decaying faster than the others. This test also helps interpret later load and cycling behavior because resting divergence can shift the initial SOC distribution prior to discharge.

Group Cycling Test Before and After Implementing Balance Control

To evaluate the developed balancing control strategies, modules were tested by conducting charging-discharging cycle tests. The developed balance control algorithms were implemented to test their effectiveness. Each cycle still consisted of CC–CV charge to the module’s upper voltage limit, rest, and CC discharge to the cutoff window. Cycling was performed for a fixed number of cycles. Throughout cycling, individual cell voltages were monitored continuously to track divergence.

4.3 Preliminary Results and Current Status

Battery cell acquisition and baseline preconditioning are complete, while active cell balancing experiments are ongoing. Initially, individual cell voltage curves were recorded during controlled charge and discharge cycles to establish baseline electrochemical behavior and confirm consistency.

To validate the testing equipment and data logging infrastructure, preliminary self-discharge screening was performed on a baseline group of EV NiMH cells (Figure 22). These profiles show stable behavior within expected limits and successfully identified cells with abnormal self-discharge rates, validating the screening protocol. Self-discharge testing of the primary EV Li-ion cells is currently underway.

In parallel, single-cell impedance characterization and galvanostatic cycling tests were conducted on the Li-ion cells (Figure 23) to measure internal resistance and capacity retention. Repeated three times per cell to ensure repeatability, these measurements provide the baseline data needed to classify cells as "nominal" or "degraded" before module assembly. This dataset also serves as an empirical model to validate the simulation findings from Section 3. While the MATLAB/Simulink models assume a uniform internal resistance for all cells, this empirical data captures actual resistance values and cell-to-cell variations, enabling a direct comparison between idealized simulation assumptions and physical reality.

Active balancing trials for the three topologies—capacitor-based, inductor-based, and Dual Active Bridge (DAB) DC–DC converter-based—are currently in progress. These trials measure state-of-charge (SOC) convergence time, voltage stability under load, and round-trip energy efficiency under identical operational parameters. Full experimental results, comparative metrics, and validation of the simulation models will be presented in future work.

These experimental and modeling results will contribute valuable hardware-validated data to the literature, where comparative evaluations of active balancing topologies under controlled conditions remain limited. Completing this hardware validation is critical to establishing the practical applicability of the proposed battery management system (BMS) design recommendations and topology selection framework.

These experimental and modeling findings are expected to constitute an important contribution to the field, as hardware-validated comparisons of active balancing topologies under controlled laboratory conditions remain limited in the published literature. Hardware validation of simulation models is a critical step in establishing the practical applicability of BMS design recommendations, and the completion of this testing will directly strengthen the evidence base for the topology selection guidance provided in this report.

5. Summary & Conclusions

This report presented a comprehensive study of active cell balancing technologies for lithium-ion battery systems used in electric vehicles (EVs), focusing on circuit topologies, control strategies, and system-level performance trade-offs. Cell imbalance—caused by manufacturing tolerances, aging, thermal gradients, and operating conditions—was shown to be a primary factor limiting battery safety, usable capacity, and service life, underscoring the need for advanced active balancing solutions within modern battery management systems (BMS). A systematic evaluation of major active balancing architectures was conducted, including switched-capacitor, inductor-based, transformer-isolated, and DC–DC converter–based topologies. Capacitor-based approaches offer simplicity and low cost but suffer from slow equalization and diminishing effectiveness at small voltage differences, restricting their suitability for large EV packs. Inductor-based balancing improves equalization speed and controllability but introduces challenges related to sequential energy transfer, magnetic losses, and electromagnetic interference. Converter-based architectures, particularly dual active bridge (DAB) systems, demonstrated superior performance for high-power applications by enabling bidirectional energy transfer, galvanic isolation, and precise control through phase-shift modulation.

Simulation results using MATLAB/Simulink for two-cell and four-cell configurations validated these analytical findings. Both inductor-based and DAB-based balancing significantly accelerated state-of-charge convergence and stabilized cell voltages under dynamic conditions. DAB-based systems, in particular, showed strong scalability and efficiency advantages by enabling direct energy transfer between cells without intermediate dissipation, making them well-suited for high-voltage and safety-critical EV battery systems. Beyond circuit performance, the report highlighted the broader impacts of effective cell balancing, including reduced energy consumption, improved charging efficiency, decreased stress on electrical grid infrastructure, extended battery service life, lower lifecycle costs, and enhanced environmental sustainability. These system-level benefits position advanced balancing strategies as a key enabler for large-scale transportation electrification.

To build upon these simulation models, a physical battery testing framework is currently underway as a primary avenue of investigation. Baseline cell characterization is already complete, where preconditioning cycles established repeatable electrochemical starting points for each cell, and preliminary self-discharge screening successfully isolated degraded cells suitable for constructing intentionally imbalanced modules. While self-discharge testing of the main Li-ion cells is actively progressing, the immediate next step in the experimental protocol involves executing active balancing trials to compare the physical capacitor-based, inductor-based, and DAB-based hardware topologies under controlled laboratory environment settings. These upcoming empirical results will serve to validate the MATLAB/Simulink findings and provide an empirically grounded baseline for topology selection recommendations.

In parallel with this ongoing hardware validation, intelligent, data-driven BMS architectures represent a critical, long-term trajectory for the field. Notably, the development of Digital Twin technology is currently underway across the industry to shift past traditional, rule-based balancing towards highly predictive, real-time operations. Creating a physics-informed virtual replica of the physical battery pack allows a BMS to perform continuous state estimation and track uneven cell degradation under highly variable real-world driving patterns. When combined with emerging Artificial Intelligence (AI) and machine learning techniques—such as adaptive control or reinforcement learning—these active Digital Twin frameworks present a compelling pathway to dynamically coordinate balancing actions, thermal management, and power electronics control while accounting for non-linear cell aging and operational uncertainty.

Ultimately, no single active balancing topology is universally optimal. Effective BMS design requires application-specific trade-offs among performance, cost, complexity, and safety, supported by integrated control strategies and emerging digital intelligence. The results of this report provide both technical guidance for engineers optimizing circuit selection and educational value for stakeholders supporting the development of safer, more efficient electric vehicle infrastructure.

Appendix A

A. MATLAB Code

```
%Two Cell balancing
function [s1,s2] = fcn (SOC1,SOC2,PWM)
  tolerance = 0.5; % 0.5% SOC difference required to switch
  if (SOC1 - SOC2) > tolerance
    s1 = PWM;
    s2 = 0;
  elseif (SOC2 - SOC1) > tolerance
    s1 = 0;
    s2 = PWM;
  else
    % Keep previous state or stay off to prevent chattering
    s1 = 0;
    s2 = 0;
  end
end
% Four cells balancing
function [s1, s2, s3, s4] = fcn(SOC1, SOC2, SOC3, SOC4, PWM)
  % Create a vector of all SOC values
  SOCVEC = [SOC1 SOC2 SOC3 SOC4];
  % Find the minimum and maximum SOC values
  minSOC = min(SOCVEC);
  maxSOC = max(SOCVEC);
  % Define the deadband for balancing (0.2%)
  deadband = 0.002;
  % Initialize all switch signals to 0 (off)
  s1 = 0; s2 = 0; s3 = 0; s4 = 0;
  % Determine which cell has the minimum SOC and activate others
  if (SOC1 < SOC2) && (SOC1 < SOC3) && (SOC1 < SOC4)
    s1 = 0;
    s2 = PWM;
    s3 = PWM;
```

```
        s4 = PWM;
    elseif (SOC2 < SOC1) && (SOC2 < SOC3) && (SOC2 < SOC4)
        s1 = PWM;
        s2 = 0;
        s3 = PWM;
        s4 = PWM;
    elseif (SOC3 < SOC1) && (SOC3 < SOC2) && (SOC3 < SOC4)
        s1 = PWM;
        s2 = PWM;
        s3 = 0;
        s4 = PWM;
    elseif (SOC4 < SOC1) && (SOC4 < SOC2) && (SOC4 < SOC3)
        s1 = PWM;
        s2 = PWM;
        s3 = PWM;
        s4 = 0;
    % If the cells are already within the deadband, turn off all balancing
    elseif maxSOC - minSOC < deadband
        s1 = 0;
        s2 = 0;
        s3 = 0;
        s4 = 0;
    end
end
```

Bibliography

Adebowale, Oluwapelumi Joseph. 2025. “Battery Module Balancing in Commercial EVs: Strategies for Performance and Longevity.” *Int J Eng Technol Res Manag* 9 (4): 162.

Ashraf, Ahmad, Bilal Ali, Mujtaba Sunjury, and Merhawi Tesfu Haile. 2025. “A Comprehensive Review of the Art of Cell Balancing Techniques and Trade-offs in Battery Management Systems.” *Energies* 18 (13): 3321. https://doi.org/10.3390/en18133321.

Attia, Peter M., Erin Moch, and Patrick K. Herring. 2025. “Challenges and Opportunities for High-Quality Battery Production at Scale.” *Nature Communications* 16 (1): 611. https://doi.org/10.1038/s41467-025-55861-7.

Bai, Hua, Jonas Kuprat, Catalina Osorio, Chunlei Liu, Marco Liserre, and Fei Gao. 2024. “Digital Twins for Modern Power Electronics: An Investigation into the Enabling Technologies and Applications.” *IEEE Electrification Magazine* 12 (3): 50–67.

Bennett, Robert. 2024. National Electric Vehicle Infrastructure Formula Program (NEVI) Brief for State Public Utility Commissions. Washington, DC: National Association of Regulatory Utility Commissions. https://doi.org/10.2172/2589511.

Deshmukh, Rohit S., Pavol Bauer, and Hadi Vahedi. 2024. “High-Accuracy Generalized Average Model of Dual Active Bridge Converters.” *IEEE Open Journal of Power Electronics* 5: 452–460. https://doi.org/10.1109/OJPEL.2024.3382808.

Dunn, Jennifer B., Linda Gaines, Jarod C. Kelly, Catlin James, and Kevin G. Gallagher. 2015. “The Significance of Li-Ion Batteries in Electric Vehicle Life-Cycle Energy and Emissions and Recycling’s Role in Its Reduction.” *Energy & Environmental Science* 8 (1): 158–168.

Engel, Hauke, Russell Hensley, Stefan Knupfer, and Shivika Sahdev. 2018. “Charging Ahead: Electric-Vehicle Infrastructure Demand.” *McKinsey Center for Future Mobility* 8.

Erickson, Robert W., and Dragan Maksimovic. 2001. *Fundamentals of Power Electronics.* 2nd ed. Norwell, MA: Kluwer Academic Publishers.

Feng, Xuning, Dongsheng Ren, Xiang He, and Minggao Ouyang. 2020. “Mitigating Thermal Runaway of Lithium-Ion Batteries.” *Joule* 4 (4): 743–770. https://doi.org/10.1016/j.joule.2020.02.010.

Gregory J. Offer, Vladimir Yufit, David A. Howey, Billy Wu, and Nigel P. Brandon, "Module Design and Fault Diagnosis in Electric Vehicle Batteries," *Journal of Power Sources* 206 (2012): 383–392.

Hein, Thomas, Daniel Oeser, Andreas Ziegler, Daniel Montesinos-Miracle, and Ansgar Ackva. 2023. "Aging Determination of Series-Connected Lithium-Ion Cells Independent of Module Design." *Batteries* 9 (3): 172. https://doi.org/10.3390/batteries9030172.

International Energy Agency. 2024. *Global EV Outlook 2024.* Paris: IEA Publications. https://www.iea.org/reports/global-ev-outlook-2024.

Khalid, Mohd Rizwan, Mohammad Saad Alam, Adil Sarwar, and M. S. Jamil Asghar. 2019. "A Comprehensive Review on Electric Vehicles Charging Infrastructures and Their Impacts on Power-Quality of the Utility Grid." *eTransportation* 1: 100006.

Lee, Wai Chung, David Drury, and Phil Mellor. 2011. "Comparison of Passive Cell Balancing and Active Cell Balancing for Automotive Batteries." In *2011 IEEE Vehicle Power and Propulsion Conference*, IEEE.

Li, Hailong, Chong Wen Ooi, Zhilin Jia, Lynda Ammar, and Mustafa Ishak. 2025. "A Review of Active Cell Balancing Methods in Electric Vehicles." *Energy Conversion and Management: X* 28: 101244. https://doi.org/10.1016/j.ecmx.2025.101244.

MathWorks. 2024. *MATLAB/Simulink (R2024b).* Natick, MA: The MathWorks, Inc.

Muhammetoglu, Batuhan, and Muhammad Jamil. 2024. "Dual Active Bridge Converter with Interleaved and Parallel Operation for Electric Vehicle Charging." *Energies* 17 (17): 4258. https://doi.org/10.3390/en17174258.

Njoku, Joseph, Emeka Nkoro, Chibueze Nwakanma, Jaehyun Lee, and Dongsoo Kim. 2025. "Leveraging Digital Twin Technology for Battery Management: A Case Study Review." *IEEE Access* 13: 21382–21412. https://doi.org/10.1109/access.2025.3531833.

Omariba, Zachary Bosire, Lijun Zhang, and Dongbai Sun. 2019. "Review of Battery Cell Balancing Methodologies for Optimizing Battery Pack Performance in Electric Vehicles." *IEEE Access* 7: 129335–129352.

Pascual, Carlos, and Philip T. Krein. 1997. "Switched Capacitor System for Automatic Series Battery Equalization." In *Proceedings of the IEEE Applied Power Electronics Conference and Exposition,* 848–854. IEEE.

Qi, Jian, and Dylan Dah-Chuan Lu. 2014. "Review of Battery Cell Balancing Techniques." In *2014 Australasian Universities Power Engineering Conference (AUPEC)*, IEEE.

Safari, Ashkan, Hoda Sorouri, Arman Oshnoei, and Frede Blaabjerg. 2025. "A State-of-the-Art Review on Battery Cell Balancing Strategies." *Discover Energy* 5 (1): 31. https://vbn.aau.dk/ws/portalfiles/portal/795283423/Final_Version_2025.pdf.

Song, Hanlu, Branislav Hredzak, and John Fletcher. 2025. “Inductor-Based Active Balancing Topology with Wide Voltage Range Capability.” *Batteries* 11 (2): 77. https://doi.org/10.3390/batteries11020077.

Sultan, Yara A., Abdelfattah A. Eladl, Mohamed A. Hassan, and Samah A. Gamel. 2025. “Enhancing Electric Vehicle Battery Lifespan: Integrating Active Balancing and Machine Learning for Precise RUL Estimation.” *Scientific Reports* 15 (1): 777.

Wood, Eric, Brennan Borlaug, Matthew Moniot, Dong-Yeon Lee, Yanbo Ge, Fan Yang, and Zhaocai Liu. 2023. *The 2030 National Charging Network: Estimating U.S. Light-Duty Demand for Electric Vehicle Charging Infrastructure*. Golden, CO: National Renewable Energy Laboratory. Report No. NREL/TP-5400-85654. https://doi.org/10.2172/1988020.

Yang, Zhijie, Haibo Huang, and Feng Lin. 2022. “Sustainable Electric Vehicle Batteries for a Sustainable World: Perspectives on Battery Cathodes, Environment, Supply Chain, Manufacturing, Life Cycle, and Policy.” *Advanced Energy Materials* 12 (26): 2200383.

Ye, Yuang, and Ka Wai Eric Cheng, 2016. “An Automatic Switched-Capacitor Cell Balancing Circuit for Series-Connected Battery Strings.” *Energies* 9 (3): 138. .

Yildirim, Bortecene, Mohammed Elgendy, Andrew Smith, and Volker Pickert. 2019. “Evaluation and Comparison of Battery Cell Balancing Methods.” In *2019 IEEE PES Innovative Smart Grid Technologies Europe (ISGT-Europe),* 1–5. IEEE.

Zhao, Zhe, Haiqiang Hu, Zhiyuan He, Hao Ho, Pooya Davari, and Frede Blaabjerg. 2023. “Power Electronics-Based Safety Enhancement Technologies for Lithium-Ion Batteries: An Overview from Battery Management Perspective.” *IEEE Transactions on Power Electronics* 38 (7): 8922–8955.

About the Authors

Woonki Na, PhD

Dr. Na received his B.S. and M.S. in electrical engineering from Kwangwoon University, Seoul, South Korea, in 1995 and 1997, respectively, and earned his Ph.D. degree in electrical engineering from the University of Texas at Arlington in May 2008. From 2008 to 2009, he was with Caterpillar Inc, Peoria, IL and participated in several hybrid electric drives programs as a Senior Engineer. From 2009 to 2010, he was a post-doctoral researcher at the University of Michigan–Dearborn. He was an Assistant Professor in the Department of Electrical and Computer Engineering, Bradley University, Peoria, IL between August 2010 and July 2013. Since August 2013, he has been a Professor in the Department of Electrical and Computer Engineering, California State University, Fresno, and he is a senior member of IEEE. His research interests include power electronics, power systems, electric drives, and digital signal process (DSP)–based control designs for hybrid electric vehicle and renewable/ alternative energy applications.

Yuanyuan Xie, PhD

Dr. Yuanyuan Xie is an Associate Professor in the Department of Mechanical Engineering at California State University, Fresno. He earned his doctorate degree from the University of South Carolina, Columbia, in 2013. His research spans from transport phenomena, energy storage and conversion, and modeling. Dr. Xie has produced more than 30 journal articles and is a member of the Electrochemical Society, the American Society of Mechanical Engineering, and the American Chemical Society.

MINETA TRANSPORTATION INSTITUTE